Chemical Geology 445 (2016) 68–83

Contents lists available at ScienceDirect

Chemical Geology

journal homepage: www.elsevier.com/locate/chemgeo

U-series isotopic signatures of soils and headwater streams in a semi-arid complex volcanic terrain

David Huckle [a], Lin Ma [b,*], Jennifer McIntosh [a], Angélica Vázquez-Ortega [c], Craig Rasmussen [d], Jon Chorover [d]

[a] University of Arizona, Department of Hydrology and Water Resources, Tucson, AZ 85721, United States
[b] University of Texas at El Paso, Department of Geological Sciences, El Paso, TX 79968, United States
[c] University of Notre Dame, Department of Civil & Environmental Engineering & Earth Science, Notre Dame, IN 46556, United States
[d] University of Arizona, Department of Soil, Water & Environmental Science, Tucson, AZ 85721, United States

ARTICLE INFO

Article history:
Received 16 July 2015
Received in revised form 28 March 2016
Accepted 5 April 2016
Available online 20 April 2016

Keywords:
Soil formation
Stream chemistry
Volcanic ash
Chemical weathering
U-series isotopes
Critical zone

ABSTRACT

Uranium-series isotopes are emerging as a tool to characterize weathering and soil forming processes in the Critical Zone. This study seeks to understand the behavior of U-series isotopes during chemical weathering and soil formation in the semi-arid and lithologically complex volcanic terrain (rhyolitic volcaniclastics and tuff) of the Valles Caldera, New Mexico (USA). A comprehensive set of samples from the Jemez River Basin Critical Zone Observatory, including bedrock, soils, dust, soil sequential extracts, soil pore water, spring water, and stream water, was systematically investigated. ($^{234}U/^{238}U$) values measured in four soil profiles ranged from 0.90 to 1.56 and ($^{230}Th/^{238}U$) values ranged from 0.48 to 1.39. Significant ^{230}Th enrichment in shallow soil profiles was interpreted as evidence of mixing with ^{230}Th-enriched volcanic ash during soil formation. Evidence of past episodic mixing of volcanic ash in these soils suggests modeling soil formation using a mass balance approach without considering possible atmospheric inputs is problematic, and future applications of existing models in heterogeneous volcanic soils should be applied cautiously. Significant ^{234}U enrichment in one soil profile was interpreted as evidence of addition of U to soils from ^{234}U-enriched soil solutions. Soil sequential extraction confirms that most of the U is contained in organo-metal colloid and exchangeable forms in shallow soils of this profile.

U-series isotopes have also shown promise as a tracer of water residence time and mixing of different water sources. In this study, ($^{234}U/^{238}U$) ratios for dissolved U are used to trace seasonal variation in source water contributions to stream flow in a small (3.29 km^2), headwater catchment within the Valles Caldera. Systematically lower ($^{234}U/^{238}U$) values (ranging from 1.7 to 2.8) were observed in dissolved U in spring and stream waters during snowmelt compared to dry seasons (($^{234}U/^{238}U$) ranging from 1.9 to 3.1) in conjunction with greater contributions of deeper groundwater sources as suggested by major element tracers Cl and Si. The lower ($^{234}U/^{238}U$) values in deeper groundwater, in contrast to previous studies, were attributed to progressive depletion of easily-weathered ^{234}U with increasing duration of water-rock interaction and increasing chemical dissolution. Further studies with more quantitative age tracers, such as ^{3}H, could help to establish the influence of residence time on stream source waters' ($^{234}U/^{238}U$) values. If established, ($^{234}U/^{238}U$) could be a powerful tracer of water sources and residence time in stream waters at the catchment scale.

1. Introduction

Chemical weathering is an important earth surface process that transfers nutrients from earth materials to the biosphere, forms soils with capacities for water retention, ion exchange and carbon stabilization, and provides a drawdown of atmospheric CO_2 over geologic timescales (e.g., Berner et al., 1983). Understanding controls on chemical weathering and soil formation rates is important to determine long term landscape evolution and sustainability of the critical zone, the dynamic region of Earth's surface where bedrock, water, soil, and life interact (e.g., Chorover et al., 2011). Specifically, quantifying the rate at which soils are produced at the weathering front vs. the rate they are eroded at the land surface is crucial to evaluate the sustainability of soil resources, which support human civilization in an era of changing climate and ever growing population (e.g., Brantley et al., 2007; Dosseto et al., 2011, 2012; Montgomery, 2007; Wilkinson and McElroy, 2007).

Fueled by recent advances in analytical techniques and mass balance models, uranium-series (U-series) isotopes are an emerging and potentially powerful tool for characterizing weathering processes in the critical zone at both long (millennial) and short (decadal to centennial) time scales. In weathering profiles, U-series isotopes have been used to calculate soil production rates and soil particle residence times (Chabaux et al., 2003a, 2003b, 2008, 2013; Dequincey et al., 2002; Dosseto et al.,

* Corresponding author.
E-mail address: lma@utep.edu (L. Ma).

http://dx.doi.org/10.1016/j.chemgeo.2016.04.003
0009-2541/

2008, 2012; Handley et al., 2013; Ma et al., 2010, 2013; Mathieu et al., 1995; Porcelli and Swarzenski, 2003). These residence times represent the time it takes since onset of chemical weathering for a soil particle to move upward (relatively) towards the surface in a soil profile before being eroded at the surface. Although there is a scientific consensus on the use of current U-series isotope mass balance models to calculate soil production rates and residence times, great care must be taken to correctly interpret time information when applied to specific systems (Chabaux et al., 2011). More studies in soil profiles across ranges of climate and lithology are needed to better establish the use of U-series modeling in weathering studies and to generate a broader dataset to document the behavior of U-series isotopes (e.g. Chabaux et al., 2008; Keech et al., 2013). Several recent U-series studies have focused on soils in granitic terrains and shale bedrock (e.g. Dequincey et al., 2002; Ma et al., 2010; Mathieu et al., 1995), while few have focused on other terrains, such as volcanic soils (Dosseto et al., 2012). Additionally, most previous studies have often focused on humid tropical or temperate climates, with few studies focusing on water-limited regions (e.g. Dosseto et al., 2012). Due to the wide occurrence of water-limited regions and the important role of volcanic soils in chemical weathering processes, studies of such systems will provide an important end-member to understand the behavior of U-series isotopes across ranges of climate and lithology.

U-series isotopes also show promise in understanding shorter-term weathering processes and modern hydrologic partitioning (e.g., Chabaux et al., 2008; Bagard et al., 2011; Maher, 2011; Maher et al., 2014; Robinson et al., 2004). The U-series composition of stream waters has been used to calculate the contribution of different water sources, such as deep and shallow groundwater, to stream flow (e.g., Bagard et al., 2011; Durand et al., 2005; Riotte and Chabaux, 1999; Schaffhauser et al., 2014). Although many studies have focused on the U-series isotope composition of large river systems to understand basin-scale erosion rates (e.g. Robinson et al., 2004; Vigier et al., 2001), few have investigated the use of U-series isotopes as a tracer of different water sources to stream flow in small headwater catchments (Schaffhauser et al., 2014), especially in semi-arid regions where stream flow generation is greatly affected by water sources with different residence time and various flow paths (e.g. Liu et al., 2008a, 2008b).

This study aims to understand the controls on U-series signatures of soils in an un-channeled, zero order basin (ZOB) on Redondo Dome in the Valles Caldera National Preserve (VCNP), in northern New Mexico, in order to investigate the applicability of U-series mass balance models to calculating soil formation rates in this complex volcanic terrain (rhyolitic volcaniclastics and tuff) under a sub-humid climate. Given the complex volcanic setting of the VCNP, our objective was to characterize the U-series composition of soils on Redondo Dome, under the influence of mixing with atmospheric dust and, potentially, volcanic ash, in addition to chemical weathering processes. We also investigated the behavior of U-series isotopes in spring and stream waters over a one year period (May 2012 to November 2012) at the catchment scale in the La Jara stream basin, a small headwater catchment draining Redondo Dome (containing the ZOB mentioned above nested within it), in order to evaluate the potential of using U-series isotopes, combined with major element chemistry, as indicators of seasonal variation in residence time and source water contributions to stream flow at the small catchment scale.

2. Background

In unweathered bedrock older than ca. 1 Ma, the ^{238}U decay series in a closed system operates at secular equilibrium, where the activity ($=\lambda N$, where N is number of atoms and λ is the isotope's decay constant) of each isotope is equal. ^{238}U decays with a half-life ($T_{1/2}$) of 4.5 Gyr to produce short-lived ^{234}Th ($T_{1/2} = 24.1$ d), then ^{234}Pa ($T_{1/2} = 6.70$ h), ^{234}U ($T_{1/2} = 244$ kyr), and ^{230}Th ($T_{1/2} = 75$ kyr). During water-rock interaction, physical and chemical processes preferentially remove different U and Th isotopes from the system, disturbing the secular equilibrium and causing variations in activity ratios of ($^{234}U/^{238}U$) and ($^{230}Th/^{238}U$) (parentheses denote activity ratios hereafter). For example, the recoil force of daughter ^{234}Th (and ^{234}U) when ejected from its parent ^{238}U during alpha decay creates $^{234}U/^{238}U$ isotope fractionation during weathering. The ^{234}Th atom may be ejected from a soil particle directly into a fluid phase, or into an adjacent soil grain, damaging the mineral lattice and making daughter isotope ^{234}U more easily removed from the solid phase during chemical weathering (e.g. Fleischer, 1982). Both of these mechanisms contribute to the preferential release of ^{234}U over ^{238}U to solution during weathering, although the relative importance of each is not well understood and may vary between different systems (Chabaux et al., 2008).

Furthermore, under oxic conditions U^{6+} is soluble, commonly as the UO_2^{2+} uranyl cation, and behaves conservatively in natural waters (e.g. Hodge et al., 1996), whereas Th is insoluble and tends to bind to solid surfaces (Gaillardet et al., 2005; Langmuir, 1997). Thus, the relative mobility of these U-series isotopes is thought to be $^{234}U > ^{238}U > ^{230}Th \cong ^{232}Th$ (e.g. Chabaux et al., 2003a, 2003b, 2008; Dosseto et al., 2008; Ma et al., 2010; Vigier et al., 2001). For these reasons, weathered soils tend to have ($^{234}U/^{238}U$) < 1 and ($^{230}Th/^{238}U$) > 1 while solution phases tend to have ($^{234}U/^{238}U$) > 1 and ($^{230}Th/^{238}U$) ≪ 1. The degree of disequilibrium in weathered soils and waters is dependent on the extent and duration of weathering processes, and can be used to trace the development of the weathering front of major U-bearing and soil forming minerals in a soil profile (e.g. Chabaux et al., 2003a, 2003b). U-series isotopes have been used for this purpose to estimate timescales of chemical weathering processes across a range of spatial and temporal scales in weathering clasts, soil profiles, aquifers, and river catchments (e.g., Bourdon et al., 2009; Chabaux et al., 2003a, 2003b, 2008; Dosseto et al., 2008, 2011, 2012; Handley et al., 2013; Keech et al., 2013; Ma et al., 2010; Mathieu et al., 1995; Pelt et al., 2008; Plater et al., 1994; Vigier et al., 2001, 2006). In addition to chemical weathering, other processes can influence the U-series isotopic composition of soils. Studies have shown that precipitation of U from a previously ^{234}U enriched soil water can result in soils with ($^{234}U/^{238}U$) > 1 (e.g. Andersen et al., 2013; Chabaux et al., 2008; Dosseto et al., 2012; Ma et al., 2010). Atmospheric dust deposition has also been shown to influence the U-series composition of soils, although relatively few studies have focused on this subject (e.g. Oster et al., 2012; Pelt et al., 2013).

Many previous studies have focused on the use of ($^{234}U/^{238}U$) disequilibrium signatures in water as a tracer of chemical weathering processes in aquifers and watersheds (e.g. Chabaux et al., 2003a, 2003b, 2008). ($^{234}U/^{238}U$) ratios in springs and deep groundwater have been shown to increase with increasing rock/water interaction and residence time (Kronfeld, 1974; Kronfeld et al., 1994; Osmond and Cowart, 1992; Tricca et al., 2001). High ($^{234}U/^{238}U$) ratios in deep groundwater mainly develop when groundwater flows through a redox front in the aquifer and U solubility decreases significantly under reducing conditions (e.g. Langmuir, 1997; Drever, 1997). Due to the decreased U concentrations in groundwater, the alpha recoil effects from the U-enriched aquifer matrix are enhanced, and groundwater can acquire abnormally high ($^{234}U/^{238}U$), e.g. up to ~10 in deep carbonate aquifers of Texas and South Africa (Osmond and Cowart, 1992; Kronfeld et al., 1994). Streams that receive contributions from such a deep groundwater water reservoir generally show increasing ($^{234}U/^{238}U$) along their flow paths or with increasing residence time (e.g. Riotte et al., 2003; Bagard et al., 2011; Schaffhauser et al., 2014).

In addition to flow paths and residence times, the degrees of U-series disequilibrium in surface and soil waters are also controlled by environmental factors including climatic, geological and hydrologic conditions (e.g. Chabaux et al., 2003a, 2003b, 2008; Maher et al., 2006, 2014; DePaolo et al., 2006; Robinson et al., 2004; Andersen et al., 2009; Pogge von Strandmann et al., 2010; Oster et al., 2012). For example, rivers that flow in hot and dry climates have ($^{234}U/^{238}U$) of ~2.0–3.0 due to enhanced alpha recoil by high physical weathering rates; these

relatively high values are in contrast to low ($^{234}U/^{238}U$) of 1.1–1.3 that are commonly observed in rivers from wet and warm climates with high chemical weathering rates (e.g. Kronfeld and Vogel, 1991; Kronfeld et al., 1994; Robinson et al., 2004; Andersen et al., 2007, 2009; Chabaux et al., 2003a, 2003b, 2008; Oster et al., 2012). Furthermore, near congruent weathering of minerals occurs in carbonate terrains produces ($^{234}U/^{238}U$) ratios close to unity (less preferential removal of ^{234}U), whereas incongruent weathering of granitic minerals can produce waters with elevated ($^{234}U/^{238}U$) values (e.g. Chabaux et al., 2008). Andersen et al. (2009) show that during weathering of granite, the ($^{234}U/^{238}U$) ratio of waters first increases and then decreases with increasing duration of water-rock interaction. The decreasing trend of ($^{234}U/^{238}U$) is due to the progressive removal of a finite pool of easily-weathered ^{234}U produced over time in the source material (Andersen et al., 2009). Therefore, subsurface environmental conditions (e.g., redox state, saturation index, and available aquifer surfaces for U precipitation) may play a major role in generating different U isotope fractionation trends with water/rock interactions (e.g. Maher et al., 2014). Seasonal variations in the ($^{234}U/^{238}U$) of stream and spring waters, in combination with major element tracers such as a geochemically conservative tracer (Cl) (Kirchner et al., 2010) and an indicator of residence time (Si) can shed light in understanding catchment scale heterogeneity in subsurface flow paths, water transit times, seasonal variations in water sources to stream flow (e.g. Liu et al., 2008a, 2008b).

3. Study area

This study focuses on the La Jara catchment, a small (3.29 km^2, elevation 2702–3429 m) headwater catchment draining Redondo Dome, a resurgent volcanic dome located within the VCNP in the Jemez Mountains, northwest of Albuquerque, NM (Fig. 1). Within the La Jara catchment is a zero order basin (ZOB; no stream channel; Fig. 1D) with two hillslopes of east and west-facing aspects, which is the focus of soil chemistry investigations in this study. The La Jara catchment, including

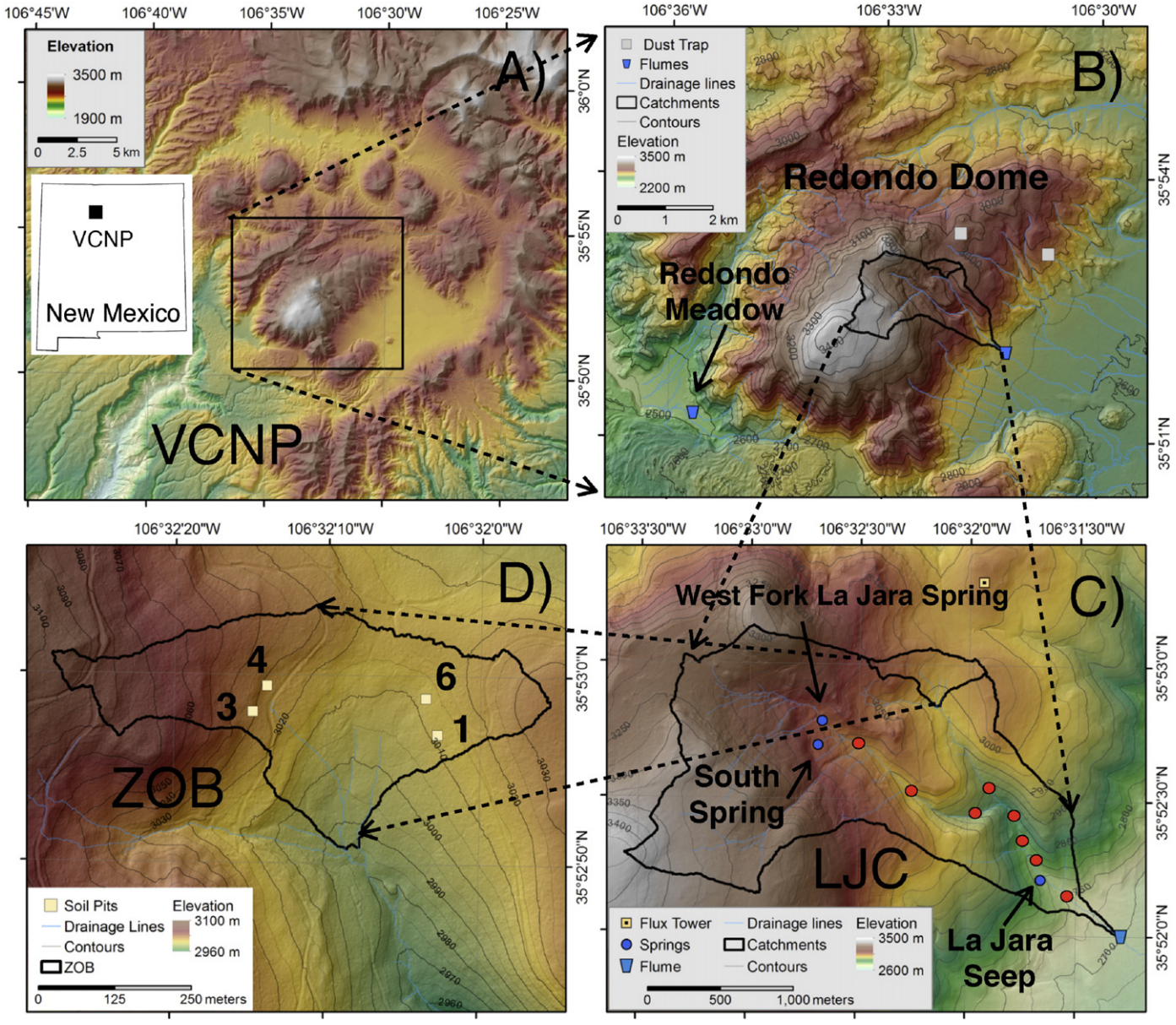

Fig. 1. Overview of the study area within the Valles Caldera National Preserve (VCNP). (A) Location of study site within VCNP in New Mexico. (B) The La Jara Catchment (LJC) is outlined on Redondo Peak. Dust traps, flux tower, LJC and Redondo Meadow flume locations are also shown. (C) The Zero-Order Basin (ZOB) is outlined within LJC. Spring and stream sampling locations are shown in blue and red circles, respectively. (D) Instrumented soil pits used in this study are shown within the ZOB. Background maps are modified from a LiDAR-derived 1 m resolution digital elevation map (Pedrial et al., 2014).

the ZOB, is part of the Jemez-River Basin Critical Zone Observatory (JRB-CZO; Chorover et al., 2011). The climate of the study area is montane and sub-humid to semi-arid with high inter-annual variability (Broxton et al., 2009). Annual temperatures average −1 °C in winter and 11 °C in summer (Zapata-Rios et al., 2015b). Snow accounts for approximately half of the annual precipitation (Gustafson et al., 2010), with an average maximum snow water equivalence of 255 mm from 1981 to 2012. The remaining precipitation falls as rain mostly during the monsoon season, and total summer precipitation around Redondo Dome varied from 245 mm to 301 mm in 2012 (Porter, 2012). Snowmelt is the dominant source of "deep" groundwater recharge in the study area (Perdrial et al., 2012; Porter, 2012). Vegetation on Redondo Dome consists of a mixed conifer forest dominated by Douglas fir, white fir, blue spruce, and aspen above 2740 m, and ponderosa pine and Gambel oak shrublands below 2740 m (Muldavin and Tonne, 2003a, 2003b).

3.1. Geological setting

The VCNP is located at the intersection of the Rio Grande Rift, which extends from the Rocky Mountains to Chihuahua, Mexico, and the Jemez Lineament, a chain of volcanic fields extending from Colorado to Arizona (Muldavin and Tonne, 2003a, 2003b). The Valles Caldera formed 1.23 Ma. After its collapse at 1.14 Ma, the caldera filled with ash and rock fragments that formed the Bandelier tuff, one of the dominant bedrock types in the VCNP (Muldavin and Tonne, 2003a, 2003b). Several resurgent and eruptive volcanic domes, including Redondo Dome, formed 54 kyr after the caldera collapsed, and there has been volcanic activity in the area as recent as 40 ka (Wolff et al., 2011). Most of Redondo Dome, including the La Jara ZOB, is underlain by Pleistocene aged rhyolitic volcaniclastics.

The dominant soils on Redondo Dome are well drained Andisols, Alfisols, Mollisols and Inceptisols (Muldavin and Tonne, 2003a, 2003b). Soils were derived from some mixture of the end-member bedrock types including the Bandelier Tuff, an older porphyritic rhyolite, volcanic ash and atmospheric dust. The bedrock within the La Jara ZOB is comprised mostly of mixed volcaniclastics including rhyolite (47%) and Bandelier Tuff (53%) that contact in the central valley of the ZOB (Supplementary Fig. A1). For this study, the aerial extents of each parent material were used to calculate a uniform ZOB-averaged parent material composition (Vazquez-Ortega et al., 2015, 2016). Although the bedrock distribution in the ZOB geologic map is relatively simple, the observed soil structures are complex. For example, Rasmussen et al. (2012) identified clear discontinuities in parent material within individual soil profiles in the ZOB (Supplementary Fig. A2). On the west-facing hillslope, the soils profiles exhibit colluvial rhyolite overlaying altered tuff, and on the east-facing hillslope the profiles are predominantly colluvial rhyolite; both hillslopes exhibited geochemical and morphologic influence of dust in the upper 5 cm of the mineral soil (Rasmussen et al., 2012; Vazquez-Ortega et al., 2015, 2016).

Previous studies on soils in the ZOB have shown that most major and trace lithogenic elements are consistently depleted relative to the ZOB averaged parent material (Porter, 2012; Vazquez-Ortega et al., 2015, 2016). However, an enrichment in Mg and Ca has been observed in some upper soil profiles, attributed to biocycling, where the surficial accumulation of decaying organic matter releases these elements to surface soils (Porter, 2012), and/or fire, which leaves Mg and Ca behind after combustion of organic matter (Chorover et al., 1994; Lavoie et al., 2010). Manganese enrichment in surface horizons was interpreted as evidence of atmospheric dust, which was highly enriched in Mn relative to the ZOB averaged parent material (Porter, 2012).

3.2. Hydrological setting

The La Jara catchment drains a southeast-facing portion of Redondo Dome and supports a perennial stream (Fig. 1C). Stream flow generation, pathways, and water transit times have been investigated for the La Jara catchment using multi-year hydrologic observations, geochemical tracers (major elements and $\delta^{18}O$), and end-member mixing models (Liu et al., 2008a, 2008b; Broxton et al., 2009; Zapata-Rios et al., 2015a, 2015b). The water end-members that contribute to stream flow in the La Jara catchment include: 1) runoff directly generated from snowmelt and monsoonal rainfall; 2) subsurface lateral flow (or shallow groundwater with similar composition to high elevation springs); and 3) deep groundwater (similar composition to low elevation springs; Fig. 1B). Direct precipitation and overland flow do not contribute significantly to stream flow (Broxton et al., 2009; Liu et al., 2008b). The subsurface lateral flow is a unique process for stream flow generation at the La Jara catchment (e.g. Liu et al., 2008a). The high elevation areas in La Jara have deep and well-drained soils (Mirand Alanos complexes; Redondo-Rubble land associations, Redondo coarse sandy loams, Redondo cobbly coarse sandy loams and Calaveras loams; Muldavin and Tonne, 2003a, 2003b; Liu et al., 2008a). The well-drained soils prevent the generation of infiltration-excess overland flow and facilitate

Table 1
Zero-Order Basin soils geochemistry.

Soil pit	Sample ID	Horizon	Depth (cm)	U (mg/kg)	Th (mg/kg)	($^{234}U/^{238}U$)	($^{230}Th/^{238}U$)	g TOC/kg soil
Pit 1	843	O	2	2.2	6.6	0.97	1.21	163.09
	844	A	10	2.6	7.3	0.96	1.05	14.01
	845	B1	30	2.3	7.6	0.95	0.99	3.05
	846	B2	46	2.4	8.5	0.91	0.98	2.75
	847	B3	76	2.4	10.6	0.92	0.87	2.25
Pit 3	854	O	2	4.9	5.8	1.56	0.48	263.50
	855	A	13	7.8	10.2	1.49	0.53	49.92
	856	AB	29	9.5	12.5	1.53	0.49	14.20
	857	B1	50	7.5	10.8	1.48	0.55	8.03
	858	B2	74	3.48	9.52	1.00	0.80	1.83
	859	B3	104	3.42	9.49	0.95	0.80	1.65
Pit 4	860	O	5	3.05	9.18	1.00	1.08	95.05
	861	A	18	3.72	11.6	0.97	1.00	29.19
	862	AB	37	3.67	10.6	0.97	0.98	28.98
	863	B	67	4.13	12.9	0.97	0.98	9.44
	864	BC	103	3.86	14.7	0.92	1.07	3.85
Pit 6	870	O	1	2.09	5.91	0.97	1.39	293.08
	871	A	10	2.6	7.39	0.98	1.02	15.69
	872	B1	31	2.34	7.03	0.96	0.98	4.52
	873	B2	50	2.26	8.22	0.90	0.93	2.89
	874	B3	79	2.77	10.9	0.95	1.01	1.74

Table 2
La Jara Zero-Order Basin bedrock and Valles Caldera National Preserve dust chemistry. NA = not analyzed.

Sample ID	Sample type	U (mg/kg)	Th (mg/kg)	($^{234}U/^{238}U$)	($^{230}Th/^{238}U$)
Rhyodacite 1	ZOB bedrock	2.7	10	NA	NA
Rhyodacite 2	ZOB bedrock	3.09	10.8	NA	NA
Rhyodacite 3	ZOB bedrock	2.94	10.2	NA	NA
White tuff 1	ZOB bedrock	3.03	19.7	NA	NA
White tuff 2	ZOB bedrock	4.4	16.6	NA	NA
White tuff 3	ZOB bedrock	4.53	15.8	NA	NA
VCNP high elev.	Dust	1.48	6.68	0.97	1.15
VCNP mid elev.	Dust	1.40	5.67	0.97	1.09

percolation of snowmelt and rainwater. The combination of high infiltration and low hydraulic conductivity of the bedrock materials generates subsurface lateral flow along the soil-bedrock interface (Liu et al., 2008a). Other deeper groundwater end-members may exist at greater depths within the Valles Caldera but do not contribute to the La Jara catchment.

The fractional contribution of these water sources to La Jara stream varies seasonally (Liu et al., 2008a; Porter, 2012). During the snowmelt season, infiltrating snowmelt creates a larger hydraulic gradient in the subsurface, pushing out greater contributions of deeper, longer residence time groundwater to stream flow under high flow conditions. This was observed as a pulse of base cations and DIC in stream flow during snowmelt in 2010. A pulse of soil-derived solutes (DOC, Al, Fe, trivalent lanthanides) was also observed in snowmelt in 2010, indicating flushing of organo-metal complexes from shallow soils during snowmelt infiltration (Vazquez-Ortega et al., 2015, 2016). During the rest of the year, stream flow is at low flow conditions and controlled by a consistent mixture of mostly shallow groundwater with some influence of deeper groundwater.

Mean transit times of waters in the La Jara catchment were estimated to be ~0.3 to 0.4 years based on oxygen and deuterium water isotopes (Broxton et al., 2009), and 5.9 to 9.6 years based on tritium analysis (Zapata-Rios et al., 2015a). These "age" ranges likely represent only a portion of the transit time distribution of La Jara waters, due to flow path heterogeneity in the subsurface (e.g. McGuire and McDonnell, 2006) and the time resolution of the tracers used.

Weathering of Ca-rich (anorthite) and Na-rich (albite) plagioclase feldspar minerals is the dominant source of base cations to La Jara stream flow (Porter, 2012). Vazquez-Ortega et al. (2015) observed positive europium anomalies in soil, soil solution, and stream water samples in the La Jara catchment, further supporting the dominance of plagioclase weathering in controlling stream solute composition. Ca/Sr

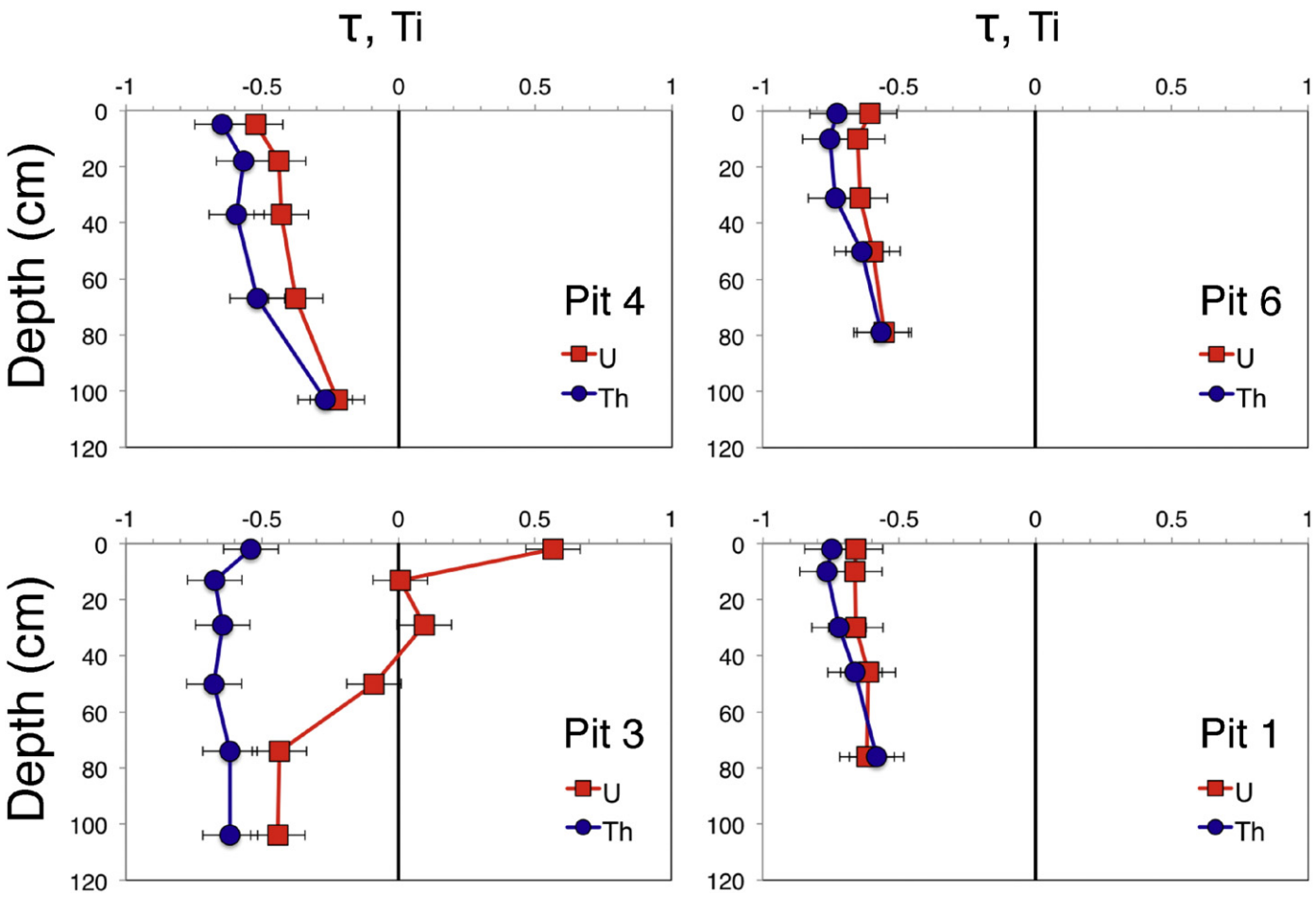

Fig. 2. Tau plots for U and Th in Zero-Order Basin soils, normalized to immobile element titanium. The vertical line at 0 represents no loss or gain of element relative to parent material. In soils from pits 1, 4, and 6 U and Th show similar depletion profiles with decreasing depth. In soils from pit 3, a strong U enrichment profile is shown with decreasing depth. This is attributed to precipitation of U from soil waters.

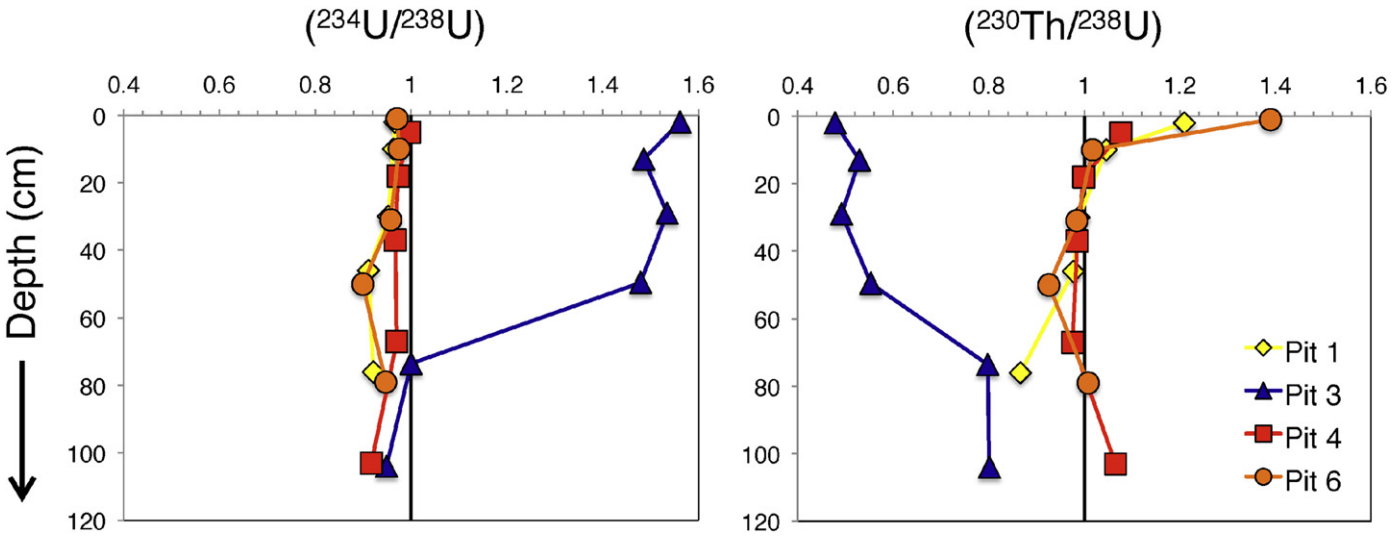

Fig. 3. ($^{234}U/^{238}U$) and ($^{230}Th/^{238}U$) in Zero-Order Basin soil pits. The vertical line at 1 represents secular equilibrium, where isotope activities are equal. ($^{234}U/^{238}U$) in soils from pits 1, 4, and 6 trend towards equilibrium with decreasing depth in the upper profiles. Soils in pit 3 display significantly enriched ($^{234}U/^{238}U$) in the upper profile. Soils in pits 1, 4, and 6 show ($^{230}Th/^{238}U$) enrichment with decreasing depth in the upper profiles likely due to mixing with volcanic ash. Soils in pit 3 show ($^{230}Th/^{238}U$) depletion with decreasing depth likely due to addition of ^{238}U. Measurement error bars are smaller than sample symbols.

ratios and Sr isotope ratios also indicated that weathering of trace disseminated calcite in La Jara soils and bedrock likely contributes solutes to stream flow, in addition to amorphous volcanic minerals likely with variable chemical composition (Porter, 2012).

4. Materials and methods

4.1. Soils

Six soil pedons were excavated forming two east–west transects across the La Jara ZOB in September of 2010. Bulk soil samples were collected by morphologic horizons, air dried, sieved to recover the <2 mm fraction, mixed until homogenous, and stored at room temperature. Total elemental concentrations (U, Th, and Ti) were analyzed using ICP-MS (Perkin Elmer DRC II, Shelton, CT) following lithium metaborate fusion (Activation Laboratories, Ancaster, Ontario), with typical errors of 2–3%.

Four soil profiles (Pedons 1, 3, 4, 6; Fig. 1D), two from each hillslope, were chosen for U-series isotopes analysis. Sample splits of the <2 mm fraction from each horizon were ground with an agate mortar and pestle and micronized with ethanol in a McCrone Mill. At the University of Texas at El Paso U-series Isotope Analytical Laboratory, ca. 100 mg of each sample were spiked with a mixed artificial ^{233}U–^{229}Th tracer for measuring U and Th isotopic ratios and concentrations. USGS rock reference standards (BCR-2 and W-2a) were analyzed along with samples for data quality assurance. Samples were fully dissolved using a three-step procedure using HNO_3–HF, $HClO_4$, and HCl–H_3BO_3 acids. U and Th were separated from solution and purified using conventional cation exchange chromatography (Ma et al., 2010; Pelt et al., 2008). U concentrations and isotopic ratios ($^{234}U/^{238}U$ and $^{233}U/^{238}U$) were measured on a Nu-plasma MC-ICP-MS using ~50 ng of U per sample. The standard-sample bracketing technique (with NBL 145B as the U bracketing solution) was used to correct for mass discrimination and drifting of ion counter/faraday cup gains during measurements. Uncertainties on U isotope ratios and U concentration were better than ~1%.

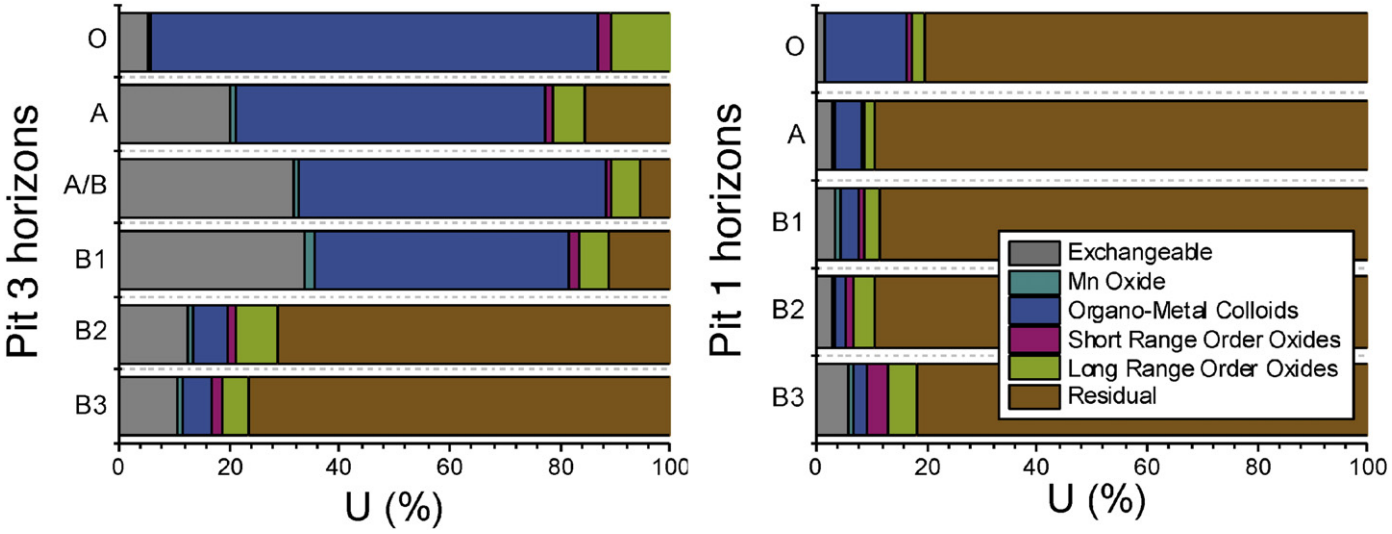

Fig. 4. U mass balance from sequential extraction analysis on soil horizons from pits 1 and 3. U% is shown in each of the targeted phases in the extraction. In soils from pit 1, most of the U is held in the residual solid phase, whereas in the upper horizons of pit 3 most of the U is held in the organo-metal colloid phase and the exchangeable phase, indicative of external U addition/precipitation processes.

Table 3
La Jara soilwater samples.

Sample ID	Soil pit	Depth (cm)	($^{234}U/^{238}U$)	U (μg/L)
G543	3	15	1.65	0.56
G544	3	38	1.66	0.89
G545	3	79	1.58	0.74
G552	1	3	1.10	0.25
G554	1	59	1.11	0.10

Measured values for W-2a were: ($^{234}U/^{238}U$) = 1.004 ± 0.004 and U concentration = 0.501 ± 0.002 ppm (n = 7; 2SD); measured values for BCR-2 were: ($^{234}U/^{238}U$) = 1.003 ± 0.001 and U concentration = 1.686 ± 0.010 ppm (n = 2; 2SD); both are in agreement with certified reference values: W-2a ($^{234}U/^{238}U$) = 1.000 and U concentration = 0.51 ± 0.01 ppm and BCR-2 ($^{234}U/^{238}U$) = 1.000 and U concentration = 1.69 ± 0.02 ppm (Sims et al., 2008). U procedural blanks were ~20 pg. The concentrations and isotope ratios ($^{229}Th/^{232}Th$ and $^{232}Th/^{230}Th$) were measured on the same instrument using ~60 ng of Th per sample, with an in-house $^{229–230–232}Th$ solution as the bracketing standard. The in-house Th solution was calibrated with IRMM 035 and IRMM 036 Th standards. Uncertainties on Th isotope ratios and Th concentration were better than 1%. Measured values for W-2a were: ($^{230}Th/^{232}Th$) = 0.712 ± 0.007 and Th concentration = 2.15 ± 0.01 ppm (n = 7; 2SD); measured values for BCR-2 were: ($^{230}Th/^{232}Th$) = 0.882 ± 0.005 and Th concentration = 5.85 ± 0.05 ppm (n = 2; 2SD); both are in agreement with certified reference values: W-2a ($^{230}Th/^{232}Th$) = 0.714 and Th concentration = 2.15 ppm and BCR-2 ($^{230}Th/^{232}Th$) = 0.877 ± 0.003 and Th concentration = 5.88 ± 0.03 ppm (Sims et al., 2008). The measured ($^{230}Th/^{238}U$) ratios for BCR2 and W-2 were 1.000 ± 0.012 and 1.001 ± 0.012, respectively. Both values are at secular equilibrium as expected. Th procedural blanks were ~40 pg.

4.2. Bedrock

Representative rock samples of the two bedrock types (Bandelier tuff and rhyolite) were crushed and unweathered rock fragments selected for mineralogical analyses by X-ray diffraction (PANalytical X'Pert Pro MPD) at the University of Arizona Center for Environmental Physics and Mineralogy and chemical analyses by X-ray fluorescence (Spectro Xepos) at the Arizona Laboratory for Emerging Contaminants (ALEC). The distribution of the two dominant parent materials in the ZOB is complex and so a weighted-average of the two rocks types was used in this study, 47% rhyolite and 53% tuff, to represent a single parent material composition for ZOB soils (Vazquez-Ortega et al., 2015a, 2016).

4.3. Dust

Atmospheric dust samples were collected at two locations in the VCNP, one high elevation site (3242 m) close to the La Jara ZOB and one mid elevation site (2825 m) on Redondo Dome (Fig. 1B). Dust traps were constructed from a circular cake pan (450 cm^2) filled with glass marbles and covered with wire mesh. The traps were secured to a metal post ~1.5 m above ground. The samples were collected over a period from Oct. 15, 2011 to Sept. 21, 2012. Both samples were subjected to lithium metaborate fusion. The mixture was placed in a 1000 °C muffle furnace and the resulting molten bead was fully dissolved in 10% HCl. The solutions were further diluted with 1% HNO_3 prior to analysis by ICP-MS (Elan DRC-II) in ALEC. U and Th concentrations and isotope ratios were measured in bulk dust samples at the University of Texas, El Paso U-series Isotope Analytical Laboratory using the procedures outlined above.

4.4. Sequential extraction of soil samples from selected excavated pedons

In order to quantify the mineral and organic components controlling the fate of U in ZOB soils, a sequential extraction scheme (Supplementary Table A1, modified after Land et al., 1999; Laveuf et al., 2012 and also employed in Vázquez-Ortega et al., 2016) was performed on soil horizons in Pedons 1 and 3. Pedon 3, located on a convex hillslope, was chosen due to its anomalously enriched ($^{234}U/^{238}U$) signatures and Pedon 1, located on a planar hillslope, was chosen for comparison. The fractionation scheme resulted in six chemically distinct fractions, namely, water soluble, adsorbed, exchangeable and carbonate bound (Step 1), reductive dissolution of Mn(IV)-oxides such as birnessite (Step 2),

Table 4
La Jara Spring and Stream Samples. BDL = below detection limit.

Sample ID	Type	Location description	Season	pH	DO (%)	Temp (°C)	($^{234}U/^{238}U$)	U (μg/L)	Si (mg/L)	Cl (mg/L)
S744	Spring	West Fork La Jara spring	Snowmelt	7.25	60.2	5.2	1.81	0.066	16.17	0.44
S745	Spring	South spring	Snowmelt	7.23	59.9	6.5	2.84	0.022	14.51	0.44
S747	Stream	1st La Jara West Fork	Snowmelt	7.64	62.7	5.2	2.18	0.031	14.76	0.37
S748	Stream	2nd La Jara West Fork	Snowmelt	7.15	62.7	5.1	2.19	0.023	14.98	BDL
S749	Stream	ZOB fork	Snowmelt	7.77	64.9	5.9	1.80	0.053	19.72	0.53
S750	Stream	1st La Jara, downstream of ZOB fork	Snowmelt	7.69	64.4	6.2	2.15	0.017	15.41	BDL
S752	Stream	2nd La Jara	Snowmelt	7.57	62.9	7	2.08	0.018	15.09	BDL
S753	Stream	3rd La Jara, upstream of Seep	Snowmelt	7.45	75	7.7	2.03	0.019	14.75	BDL
S751	Spring	La Jara seep	Snowmelt	5.62	67.5	5.6	1.94	0.024	14.72	0.47
S754	Stream	Upper La Jara flume	Snowmelt	8.16	66.4	8.4	2.03	0.015	13.52	0.38
S759	Spring	Redondo Meadow (outside La Jara)	Snowmelt	7.4	68.3	16.3	1.68	0.011	17.74	0.52
S939	Spring	West Fork La Jara spring	November	7.88	60.5	4.7	1.86	0.015	19.26	0.60
S940	Spring	South spring	November	7.39	60.5	7.3	3.09	0.003	9.38	0.38
S941	Stream	1st West Fork	November	7.55	70.1	1.9	2.52	0.006	10.04	0.57
S942	Stream	2nd West Fork	November	7.07	59.4	0.1	2.36	0.005	10.04	0.58
S943	Stream	3rd West Fork upstream of ZOB fork	November	7.12	59.5	0.1	2.40	0.005	10.21	0.60
S944	Stream	1st La Jara, downstream of ZOB fork	November	7.06	60.3	0.4	2.27	0.005	10.35	0.59
S945	Stream	2nd La Jara	November	7.17	59.8	1.4	2.23	0.006	9.41	0.77
S946	Stream	3rd La Jara, upstream of seep	November	7.48	58.5	2.2	2.16	0.006	9.43	0.76
S947	Spring	La Jara seep	November	7.25	57.2	5.1	2.27	0.004	9.09	0.47
S948	Stream	Upper La Jara flume	November	7.86	62.8	0.4	2.25	0.005	9.31	0.64
S949	Stream	Lower La Jara flume	November	7.37	60.6	0.2	2.25	0.004	8.87	0.72

Fig. 5. a. ($^{234}U/^{238}U$) values of spring and stream waters collected during May 2012 (snow melt season). Background maps are modified from a LiDAR-derived 1 m resolution digital elevation map (Pedrial et al., 2014). b. ($^{234}U/^{238}U$) values of spring and stream waters collected during November 2012 (dry season). Background maps are modified from a LiDAR-derived 1 m resolution digital elevation map (Pedrial et al., 2014).

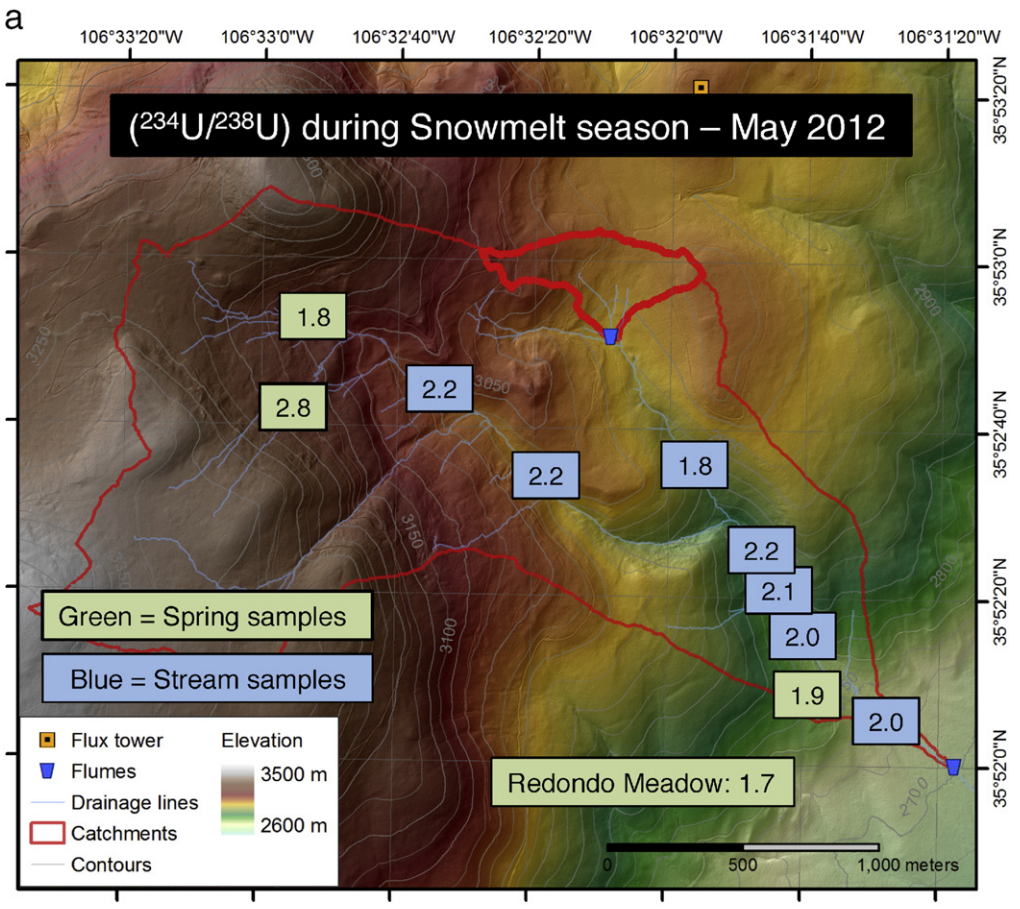
a
106°33'20"W
106°33'0"W
106°32'40"W
106°32'20"W
106°32'0"W
106°31'40"W
106°31'20"W
35°53'20"N
35°53'0"N
35°52'40"N
35°52'20"N
35°52'0"N
(234U/238U) during Snowmelt season – May 2012
1.8
2.8
2.2
2.2
1.8
2.2
2.1
2.0
1.9
2.0
Green = Spring samples
Blue = Stream samples
Redondo Meadow: 1.7
Flux tower
Flumes
Drainage lines
Catchments
Contours
Elevation
3500 m
2600 m
0
500
1,000 meters

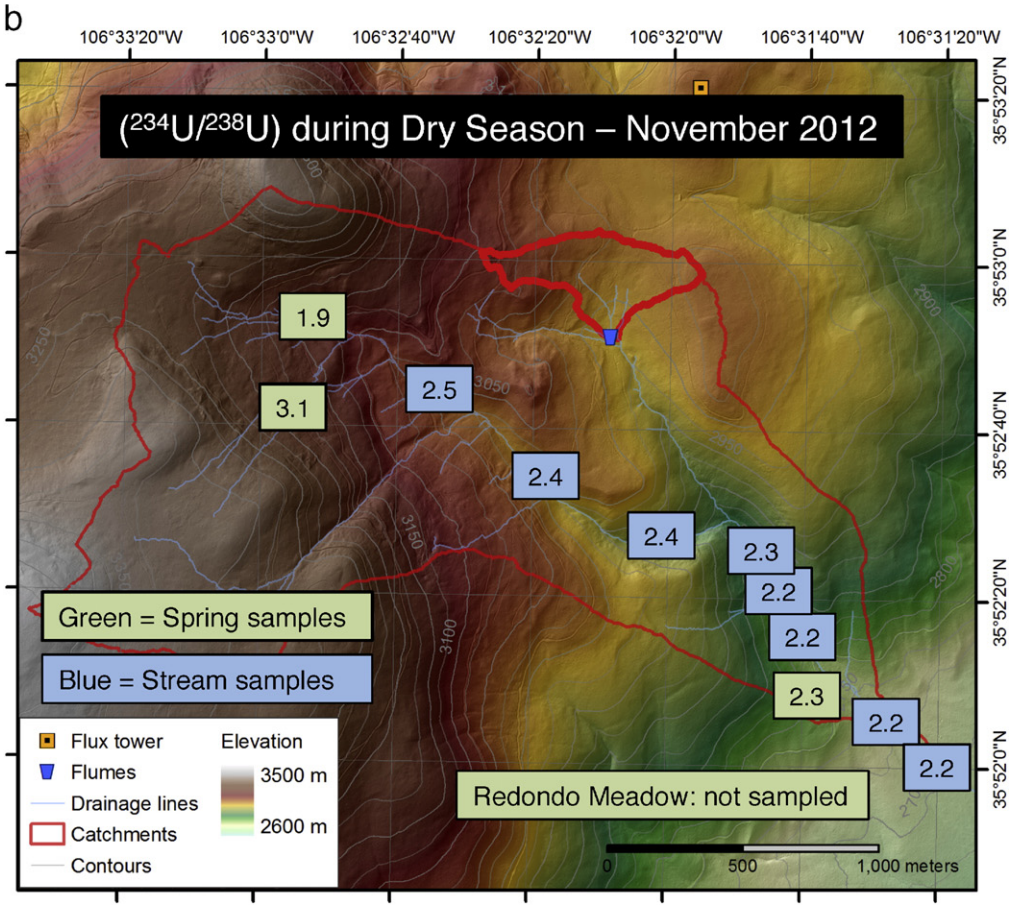
b
106°33'20"W
106°33'0"W
106°32'40"W
106°32'20"W
106°32'0"W
106°31'40"W
106°31'20"W
35°53'20"N
35°53'0"N
35°52'40"N
35°52'20"N
35°52'0"N
(234U/238U) during Dry Season – November 2012
1.9
3.1
2.5
2.4
2.4
2.3
2.2
2.2
2.3
2.2
2.2
Green = Spring samples
Blue = Stream samples
Redondo Meadow: not sampled
Flux tower
Flumes
Drainage lines
Catchments
Contours
Elevation
3500 m
2600 m
0
500
1,000 meters

dispersion of organo-metal colloids (Step 3), reductive dissolution of poorly-crystalline Fe-(oxy)hydroxides such as ferrihydrite (Step 4), reductive dissolution of crystalline Fe-(oxy)hydroxides such as goethite (Step 5), and the residual solids mainly consisting of silicates (Step 6). Sequential extractions were performed in triplicate on 1.0 g of air-dried soil, and mean values were reported. Each extraction step was followed by a rinse with DI water for 30 min with a 1:20 m/V ratio at room temperature. Extractions and rinses were shaken at 100 relative centrifugal force (rpm) speed followed by centrifugation at 44,000 rpm for 30 min and then filtered through a 0.2 μm cellulose acetate membrane. The rinses were combined into the supernatant in each extraction. The residues were then subjected to further extractions in the following steps until the sequential extraction was completed. Soil-free "blanks" for the five steps were carried out in triplicate as well and matrix affects were accounted for during analysis. Samples were diluted with 1% HNO_3 and U concentrations were analyzed via ICP-MS at ALEC.

4.5. Waters

Surface water grab samples were collected at two high elevation springs in the La Jara catchment (West Fork spring and South spring), and at various locations along La Jara stream to capture the longitudinal variability of aqueous geochemistry and U-series isotope composition. A sample was also collected from Redondo Meadow spring, a low elevation spring located outside the La Jara catchment, because it best represents the source of a deep groundwater end-member to La Jara stream (Fig. 1B, C). Grab samples were collected both in May 2012 (the spring snowmelt season) and in November 2012 (the dry season) to capture seasonal variability. Water samples were collected in combusted amber glass bottles (for carbon and anion analyses) and in acid-washed high density polyethylene (HDPE) bottles (for major cations and trace element analyses). Samples were packed on ice, shipped to the University of Arizona and filtered within 2 days of collection with 0.45 μm nylon filters. Optima grade nitric acid was added to splits for metal(loid) analyses to preserve the samples.

Passive capillary wick lysimeters (PCaps) installed at varying depths in each of the ZOB pedons (Perdrial et al., 2012) were used to collect soil solution under a constant negative pressure head of ca. 3 kPa. The PCaps consist of a fiberglass wick covered HDPE plate that is propped via turnbuckles into contact with the bottom of the soil horizon of interest. Soil solution is transmitted along the wick surface through tubing to a carboy that can be evacuated from the surface. Soil solution samples from three depths in Pedon 3 (15 cm, 38 cm, 79 cm) and one depth in Pedon 1 (3 cm) from snowmelt 2012 were included in this study and analyzed for major and trace ion chemistry and U-series isotope composition. PCaps have been shown not to sorb or release U from soil solution and thus are appropriate for the given study (Pedrial et al., 2014).

Major and minor cation concentrations, including U, for all water samples were analyzed by ICP-MS and anion concentrations were measured by IC, in ALEC at the University of Arizona. At the University of Texas El Paso U-series Isotope Analytical Laboratory, ca. 30 g of each water sample were spiked with an artificial ^{233}U tracer (NBL 111a) for measuring U concentrations and ($^{234}U/^{238}U$). Samples were then evaporated and processed using the same cation exchange procedure as for soil samples. U concentrations and isotopic ratios ($^{234}U/^{238}U$) were measured on a Nu-plasma MC-ICP-MS. For water samples, measured ($^{234}U/^{238}U$) were corrected for contribution of ^{234}U from the ^{233}U spike (NBL 111a: $^{234}U/^{233}U = 0.0019$). For data quality assurance, one replicate water sample (S754) was run without addition of the ^{233}U spike and the ($^{234}U/^{238}U$) = 2.05 ± 0.01, in agreement with the spiked S754 sample ($^{234}U/^{238}U$) = 2.03 ± 0.01.

5. Results

5.1. Bedrock, soils, dust, and soil solution

In ZOB soils (Pedons 1, 3, 4, and 6), U concentrations ranged from 2.09 to 9.50 mg kg^{-1} and Th concentrations from 6.60 to 14.7 mg kg^{-1} (Table 1). ZOB weighted averaged bedrock concentrations of U and Th were 3.48 mg kg^{-1} and 14.1 mg kg^{-1}, respectively (Table 2). U and Th concentrations in dust, averaged between high and mid elevation samplers, were 1.44 mg kg^{-1} and 6.18 mg kg^{-1}, respectively (Table 2). Th concentrations were lower in soils than in bedrock in all of the pedons, and U concentrations were lower in most soils with the notable exception of the upper horizons in Pedons 3 and 4 on the east-facing ZOB hillslope. U and Th concentrations decreased gradually from depth towards the surface of Pedons 1, 4, and 6, but showed significant increases at shallow depths in Pedon 3 (Table 1).

To quantify element depletion and enrichment in ZOB pedons relative to parent bedrock we calculated mass transfer coefficient values for U (τ) as a function of depth (e.g. Anderson et al., 2002; Brimhall and Dietrich, 1987; Brantley et al., 2007):

$$\tau_{j,w} = \left(\frac{Cj,w}{Cj,p} \times \frac{Ci,p}{Ci,w}\right) - 1 \quad (1)$$

where C is concentration of an element: j is the element of interest and i is the immobile element in weathered (w) and unweathered parent (p) material. In this study, concentrations were normalized to titanium (Ti) as an "immobile" element. Values of $\tau = 0$ indicate no change in an element's soil concentration relative to parent material, whereas $\tau > 0$ indicates enrichment and $\tau < 0$ indicates depletion in soil relative to bedrock. Depletion profiles were observed for U and Th in Pedons 1, 4, and 6: U and Th show similar depletion profiles with decreasing depth. In the surface soils of Pedons 1, 4, and 6, U and Th show large and similar loss (~50–70%) in relative to Ti, suggesting that weathering and soil formation processes have similar controls on the mobility of U and Th in these ZOB pedons. It is noted that the degree of Th loss in Pedons 1, 4, and 6 is slightly higher than the degree of U loss, probably suggesting a higher mobility of Th relative to U. The enhanced Th mobility could be due to the presence of organic complexes or loss of Th due to transport of fine particles (e.g. Ma et al., 2010). For Pedon 3, we observed significant enrichment of U at the soil surface and a progressive depletion of Th at depth with moderate enrichment at the surface (Fig. 2).

($^{234}U/^{238}U$) values ranged from 0.90 to 1.56 and ($^{230}Th/^{238}U$) values ranged from 0.48 to 1.39 in ZOB soils (Pedons 1, 3, 4 and 6). ($^{234}U/^{238}U$) values were generally less than 1 and increased towards the soil surface approaching unity (Fig. 3), with the exception again of Pedon 3, which showed strong ^{234}U enrichment (($^{234}U/^{238}U$) > 1) increasing towards the soil surface. ($^{230}Th/^{238}U$) values showed general enrichment profiles in all pedons (except Pedon 3) towards the surface (Fig. 3). In atmospheric dust, ($^{234}U/^{238}U$) values were 0.97 and ($^{230}Th/^{238}U$) ranged from 1.09 to 1.15 in middle and high elevation samples, showing less variation than soil samples (Table 2).

Sequential extractions reveal stark differences in U-bearing phases between Pedons 1 and 3 (Fig. 4). In Pedon 1, the residual solid phase was dominant in the U mass balance, whereas organo-metal colloid and exchangeable U were dominant in the upper horizons of Pedon 3 (Fig. 4), where enrichment of U (Fig. 2) and elevated ($^{234}U/^{238}U$) (Fig. 3) were also observed. The lower horizons of Pedon 3 were similar to those in Pedon 1, with the bulk of total U measured in the residual solid phase (Fig. 4). Total organic carbon concentrations in soils ranged from 1.7 to 293 g kg^{-1} and were highly enriched in the surface horizons (Table 1).

During the snowmelt season in 2012, soil solution U concentrations were higher in Pedon 3 (0.56 to 0.89 μg L^{-1}) than Pedon 1 (0.10 to 0.25 μg L^{-1}) (Table 3). Likewise, ($^{234}U/^{238}U$) values were also higher in Pedon 3 (1.58 to 1.66) relative to Pedon 1 (1.10 to 1.11).

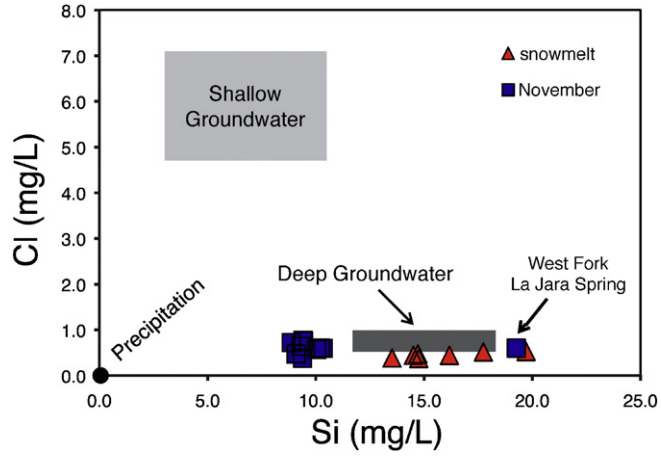

Fig. 6. Si vs. Cl concentrations of spring and stream waters from La Jara Catchment (LJC) collected during spring snowmelt and in November (dry season). Mixing endmembers of Precipitation, Shallow Groundwater (represented by La Jara soil, water and spring samples), and Deeper Groundwater (represented by Redondo Meadow samples, located outside LJC) are shown (Porter, 2012). Samples collected during the snowmelt season display a greater contribution of deeper groundwater vs. samples collected during November, with the exception of the West Fork La Jara spring. Measurement error bars are smaller than sample symbols.

5.2. Surface waters

Uranium concentrations in La Jara springs ranged from 0.022 to 0.066 μg L^{-1} during the snowmelt season in 2012 and from 0.003 to 0.015 μg L^{-1} during November 2012 (Table 4). Uranium concentration in the Redondo Meadow spring, located outside of the La Jara catchment, was 0.011 μg L^{-1} in snowmelt 2012 and was not sampled in November due to lack of flow. Dissolved ($^{234}U/^{238}U$) values in La Jara and Redondo Meadow springs ranged from 1.70 to 2.80 during the snowmelt season in 2012 (Fig. 5a). During November 2012, ($^{234}U/^{238}U$) values of La Jara springs were significantly higher, ranging from 1.90 to 3.10 (Fig. 5b). Si and Cl concentrations in La Jara springs also showed distinct seasonal variation during the snowmelt and the November dry season (Fig. 6), with the exception of West Fork spring, which had similar concentrations. During the snowmelt 2012, Si and Cl concentrations in La Jara springs and Redondo Meadow ranged from 14.51 to 17.74 mg L^{-1} and 0.44 to 0.52 mg L^{-1}, respectively. During November 2012, Si and Cl concentrations ranged from 9.09 to 19.3 mg L^{-1} and 0.38 to 0.60 mg L^{-1}, respectively for La Jara springs.

Uranium concentrations in La Jara stream ranged from 0.015 to 0.053 μg L^{-1} during the snowmelt 2012 and 0.004 to 0.006 μg L^{-1} during November 2012 (Table 4). Dissolved ($^{234}U/^{238}U$) values in La Jara stream ranged from 1.80 to 2.20 during the snowmelt 2012. During November 2012, stream ($^{234}U/^{238}U$) values were systematically higher, ranging from 2.20 to 2.50 and similar to those of the La Jara springs. Longitudinal variation in ($^{234}U/^{238}U$) values was observed along La Jara stream in both seasons; values decreasing with distance downstream and hence with decreasing elevation (Fig. 5). Si and Cl concentrations in La Jara stream waters also show distinct seasonal variation, with the snowmelt-season samples having significantly greater Si concentrations (Fig. 6). During the snowmelt 2012, Si and Cl concentrations in La Jara stream ranged from 13.52 to 19.72 mg L^{-1} and 0.37 to 0.53 mg L^{-1}, respectively, whereas during November 2012, they ranged from 8.87 to 10.35 mg L^{-1} and 0.57 to 0.77 mg L^{-1}, respectively.

6. Discussion

6.1. Influence of volcanic ash in ZOB soils

Chemical weathering typically leads to soil profiles with ($^{234}U/^{238}U$) < 1 and ($^{230}Th/^{238}U$) > 1 (Fig. 7), due the relative mobility of U-series isotopes as $^{234}U > {}^{238}U > {}^{230}Th$ (e.g. Chabaux et al., 2003a, 2003b, 2008; Dosseto et al., 2008; Ma et al., 2010; Vigier et al., 2001). The atypical trends observed in the upper profiles of ZOB soil Pedons 1, 4, and 6, with ($^{234}U/^{238}U$) values trending towards unity in surface horizons (Fig. 3) and marked ($^{230}Th/^{238}U$) enrichment in surface O-horizons (Fig. 3), are difficult to generate in the subsurface by chemical weathering alone and are interpreted to be controlled by mixing of volcanic ash and atmospheric dust into surface horizons.

Volcanic activity has occurred in the VCNP as recently as 40–55 Ka during the El Cajete series of eruptions that included a plinian type eruption of pumice and ash to form the El Cajete cone (Wolff et al., 2011). Most of the pumice and tuff from the El Cajete eruption was deposited to the east of the eruptive center (away from Redondo Dome) (Wolff et al., 2011), however it is likely that some ash was deposited on the dome given the close proximity. In addition, approximately 25 other eruptions have occurred in the Valles Caldera since its collapse 1.2 Ma that could have also contributed ash to Redondo Peak and the ZOB (Goff, 2009).

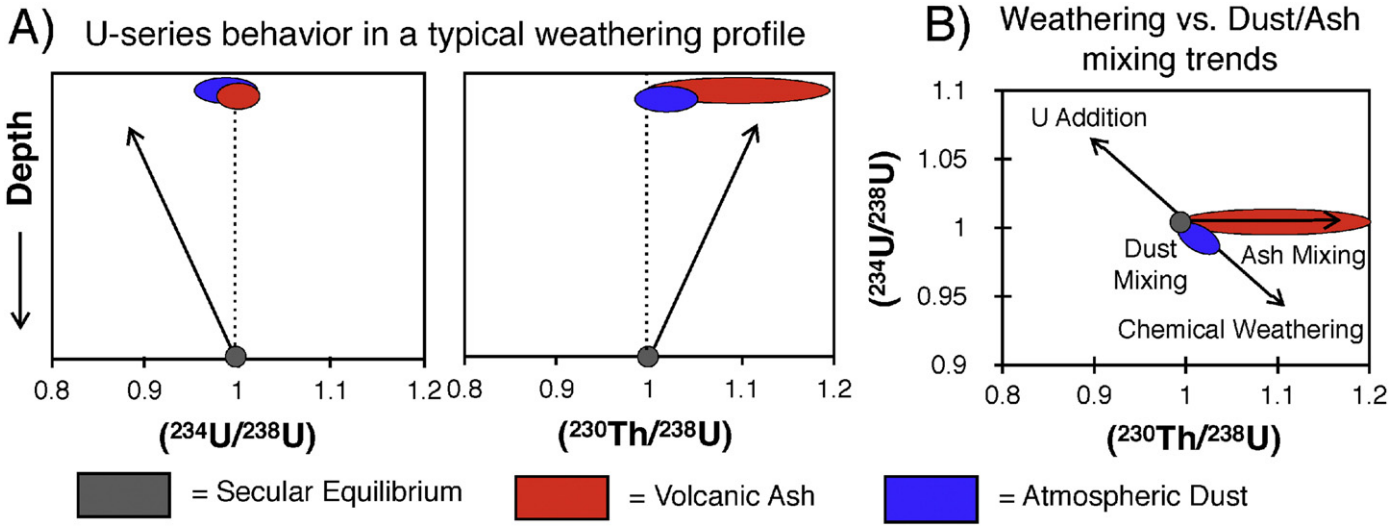

Fig. 7. Conceptual model of U-series behavior in a typical weathering profile and the effects of volcanic ash and atmospheric dust inputs. (A) Depth profiles of ($^{234}U/^{238}U$) and ($^{230}Th/^{238}U$): ($^{234}U/^{238}U$) tends to decrease and ($^{230}Th/^{238}U$) tends to increase towards the surface with progressive weathering. B) Correlation between ($^{234}U/^{238}U$) and ($^{230}Th/^{238}U$) due to hypothesized influence of volcanic ash and atmospheric dust mixing on the U-series composition of soils is shown; chemical weathering and U addition processes are also shown.

Young (<1 Ma) volcanic rocks and volcanic ash often acquire ($^{230}Th/^{238}U$) enrichment due to Th/U fractionation during magma melting prior to eruption, whereas ($^{234}U/^{238}U$) in young volcanic materials tends to be close to unity due to limited U isotope fractionation during magmatic processes (Fig. 7) (e.g. Asmerom, 1999; Nauret et al., 2012; Russo et al., 2009). Indeed, the observed U-series signatures in ZOB O-horizon soils for Pedons 1, 4, and 6, i.e. ($^{234}U/^{238}U$) ~ 1 and ($^{230}Th/^{238}U$) > 1, suggest that U and Th mass balances in shallow soils were possibly affected by mixing with volcanic ash sourced around VCNP (Fig. 8a).

Note that the hypothesized range of ($^{230}Th/^{238}U$) in common volcanic ash is 1.0 to 1.3, which is lower than some of the observed ZOB soil values (up to 1.4; Fig. 8a). Chemical weathering processes on ash-influenced soils could further increase ($^{230}Th/^{238}U$) by ^{238}U loss (e.g. Chabaux et al., 2008). High concentrations of soil organic carbon in the ZOB O-horizons likely leads to accelerated chemical weathering of mineral material by organic acids, consistent with the high ($^{230}Th/^{238}U$) enrichment observed in the O horizons of Pedons 1, 4, and 6 (Fig. 3).

Relatively high concentrations of U (1.38 mg kg^{-1}) and Th (5.82 mg kg^{-1}) measured in atmospheric dust samples collected near La Jara (Fig. 1B) suggest dust also plays a role in modifying U-series signatures and mass balances in ZOB soils. Indeed, ($^{234}U/^{238}U$) and ($^{230}Th/^{238}U$) values measured in La Jara dust samples were 0.97 and 1.10–1.20 (Fig. 8a), falling within the range of global dust U-series values compiled by Oster et al. (2012). These values are consistent with dust having originated from recently weathered soil (Fig. 8a). This suggests that the current U-series composition of ZOB surface soils is likely influenced by a combination of past episodic volcanic ash deposition, local biogeochemical weathering conditions, as well as deposition of atmospheric dust. The role of dust input in soil formation has been highlighted for arid and semiarid areas near the Valles Caldera region. For example, using $^{87}Sr/^{86}Sr$ ratios and Ca/Sr values in soils from southern New Mexico, Capo and Chadwick (1999) have demonstrated that a significant fraction of silicate mass in the uppermost 25 cm of soil profiles could be atmosphere-derived.

The U-series evidence of deposition of young (<1 Ma) volcanic ash and dust makes modeling soil formation rates in the ZOB using U-series isotopes problematic. Most U-series mass balance models assume that the evolution of a soil particle in a simple weathering profile originates from a single parent at secular equilibrium and constant input and output fluxes of U-series isotopes over time. For example, soil and saprolite formation rates were successfully determined with U-series mass balance models for mono-lithologic temperate watersheds in Australia (grano-diorite bedock) and United States (shale bedrock) (Dosseto et al., 2008; Ma et al., 2010, 2013). In both cases, local lithology was relative simple and dust inputs to surface soils were negligible (e.g. under temperate and humid climate conditions). Due to the episodic nature of ash deposition and dust inputs, we conclude that the application of U-series models that assume soil production from a single parent and constant inputs of U-series isotopes over time would be inappropriate in La Jara ZOB soils.

6.2. Influence of soil solution on U-series composition of ZOB soil Pedon 3

Values of ($^{234}U/^{238}U$) in the upper horizons of Pedon 3 exceed 1.5 (Fig. 3), which is much higher than that is typically observed in weathered soils (<1.0, e.g. Chabaux, 2008). High ($^{234}U/^{238}U$) ratios have been observed in weathering profiles and are often attributed to U sorption or precipitation into secondary Fe-oxyhydroxide minerals from ^{234}U-enriched soil solutions (e.g. Andersen et al., 2013; Chabaux et al., 2008; Dequincey et al., 2002; Dosseto et al., 2008; Ma et al., 2010). The mass transfer coefficient for U plot for Pedon 3 (Fig. 2) is also characterized as a typical addition profile (Brantley et al., 2007) with external sources of U added to soils. The complementary ($^{230}Th/^{238}U$) depletion profile (Fig. 3) could have been generated by progressive addition of ^{238}U, driving down the value of ($^{230}Th/^{238}U$).

Sequential extraction data confirm that U chemical lability or operational speciation (Fig. 4) correlates with its total and isotopic U enrichment/depletion in the ZOB soils (Figs. 2 and 3). In Pedon 1, located on a planar hillslope, silicate and phosphate mineral residuals of the sequential extraction contain most of the soil U, and U sorption to inorganic and organic surfaces, or precipitation of metal (oxyhydr)oxide secondary phases are not dominant processes (Fig. 4). However, in the upper horizons of Pedon 3, located on a convex hillslope, significant ($^{234}U/^{238}U$) enrichment is observed and a large fraction of U is observed in these more geochemically labile, organo-metal colloids and exchangeable forms (Figs. 2 and 3). Such an observation is consistent with the high affinity of uranyl cation for carboxyl ligands in soil organic matter (Chabaux et al., 2003a, 2003b), and with the prevalence of organically-complexed lanthanide series metals in the same soils (Vázquez-Ortega et al., 2016).

Shallow groundwater observed to discharge near Pedon 3 from upslope could be providing a source of ^{234}U-enriched U to upper profile soils. If we assume that the U in the upper horizons of Pedon 3 is a

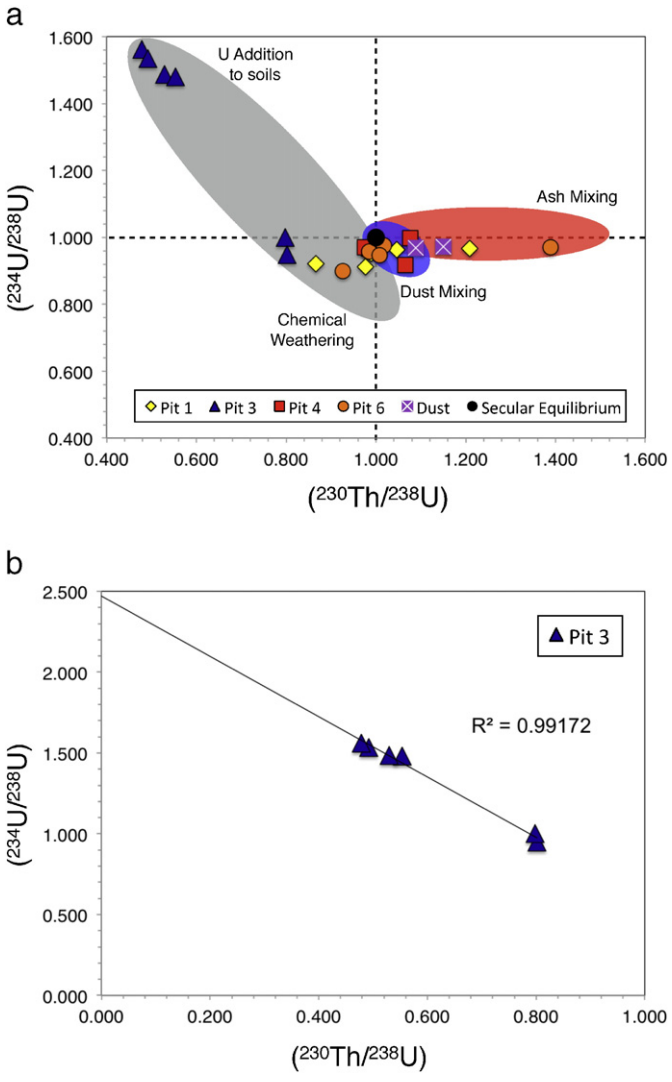

Fig. 8. a. ($^{230}Th/^{238}U$) vs. ($^{234}U/^{238}U$) on Zero-Order Basin soil samples. In pit 3 soils, the activity ratios are negatively correlated and show a trend indicative of U addition from soil solution. Soil samples from pits 1, 4, and 6 show trends indicative of mixing with volcanic ash and atmospheric dust. Measurement error bars are smaller than sample symbols. b. Hypothesized mixing line extending to a ($^{230}Th/^{234}U$) value of zero to indicate the ($^{234}U/^{238}U$) value of the shallow groundwater end member contributing dissolved U to Pit 3 soils (Th assumed insoluble). We interpolate a ($^{234}U/^{238}U$) value of ~2.5 for the shallow groundwater end member, which is consistent with ($^{234}U/^{238}U$) observed in La Jara springs (~2.2–3.1).

mixture between ^{234}U-enriched shallow groundwater and ^{234}U-depleted residual soils (e.g., lower horizons of Pedon 3), the (^{234}U/^{238}U) of the ^{234}U-enriched shallow groundwater can be inferred from the mixing trend between the upper and lower horizons in Pedon 3 (Fig. 8a). Assuming (^{230}Th/^{238}U) activity ratios in water phases equal to 0, the inferred (^{234}U/^{238}U) of the shallow groundwater for Pedon 3 is ~2.5 (Fig. 8b). Such a high (^{234}U/^{238}U) is consistent with the range of (^{234}U/^{238}U) observed for La Jara springs (~2.2–3.1) for high elevation sites near the Redondo peak (e.g. Fig. 5), suggesting that the discharge of shallow groundwater near Pedon 3 could be hydraulically linked to the springs at higher elevations. The springs at higher elevations of the La Jara catchment are characterized by high (^{234}U/^{238}U) due to easily released ^{234}U from recoil tracks in U-bearing mineral during water-rock interactions (see Section 6.3).

Soil solution from Pedon 3 had (^{234}U/^{238}U) ranging from 1.58 to 1.66 (Table 3), similar to what is observed in upper Pedon 3 soils (Table 1), but significantly lower than the inferred (^{234}U/^{238}U) of the shallow groundwater. In Pedon 1, soil solution (^{234}U/^{238}U) was relatively lower, ranging from 1.10 to 1.11, also similar to (^{234}U/^{238}U) in Pedon 1 soils (Table 1). The similar (^{234}U/^{238}U) observed for soil solution and soils in both Pedons 1 and 3 may suggest that the sampled soil solution reflects contribution only from in-situ weathering of upper horizon soils (weathered residuals) with no or limited alpha recoil effects.

It is implied that the shallow groundwater end-member with high (^{234}U/^{238}U) values (such as ~2.5) was generated from early water-rock interaction from profiles upslope and then was immobilized in pedogenic organo-mineral complexes in the upper horizons of Pedon 3. Indeed, due to its landscape position (on a convex hillslope), Pedon 3 receives greater colluvial inputs and has poorer drainage compared to Pedon 1 (on a linear hillslope). A large enrichment of REE has been observed in the upper horizons of Pedon 3, which was attributed to colluvial delivery of organic-REY complexes to this convex site (Vázquez-Ortega et al., 2016). Accumulation of organic complexes from colluvial input may lead to the enrichment in U concentration and high (^{234}U/^{238}U) ratios observed in upper Pedon 3, but not in Pedon 1. The amounts of U associated with organo-metal colloids correlate well with the (^{234}U/^{238}U) ratios in bulk soils for Pedon 3 (Fig. 9), suggesting that the organo-metal colloid component is characterized by high U/Th and high (^{234}U/^{238}U) signatures. By contrast, no such correlation is observed for Pedon 1 (Fig. 9).

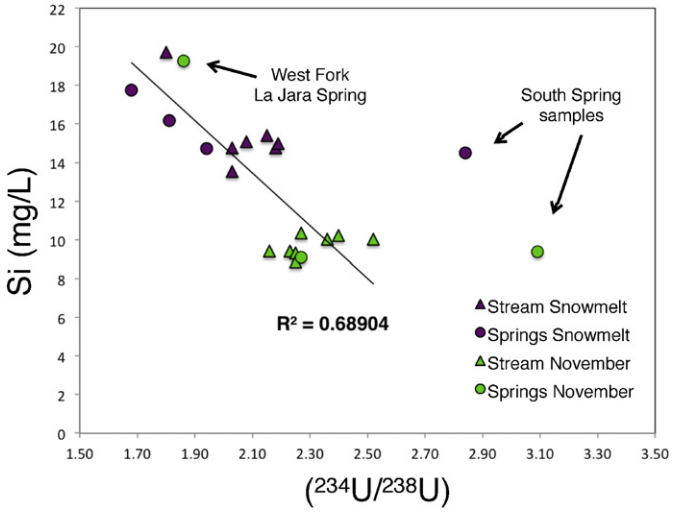

Fig. 10. Si vs. (^{234}U/^{238}U) in La Jara spring and stream samples from both the spring snowmelt and November (dry) seasons. Most samples, with the exception of the South spring samples, plot along a trend line of decreasing (^{234}U/^{238}U) with increasing Si. Snowmelt season water samples have higher Si and lower (^{234}U/^{238}U), indicating longer residence times, while dry season water samples have lower Si and higher (^{234}U/^{238}U) indicating shorter residence times. Measurement error bars are smaller than sample symbols.

6.3. ^{234}U/^{238}U ratios as an indicator of water residence time and flow path

Previous studies have suggested that the water sources contributing to stream flow in the La Jara catchment include: 1) runoff directly generated from snowmelt and monsoonal rainfall; 2) subsurface lateral flow (or shallow groundwater); and 3) deep groundwater (Broxton et al., 2009; Liu et al., 2008a, 2008b; Porter, 2012). The fractional contribution of these sources varies seasonally and spatially. In the La Jara catchment, greater Si concentrations in springs and stream waters during the snowmelt season may indicate greater contributions of deep groundwater with long residence time and flow paths to stream flow, compared to the fall dry season which has lower Si concentrations and receives less deep groundwater contribution (Fig. 6). It has been hypothesized that during the snowmelt season, infiltrating snowmelt water raises the local water table, resulting in a greater hydraulic gradient in the subsurface, thereby mobilizing older, Si-rich groundwater via

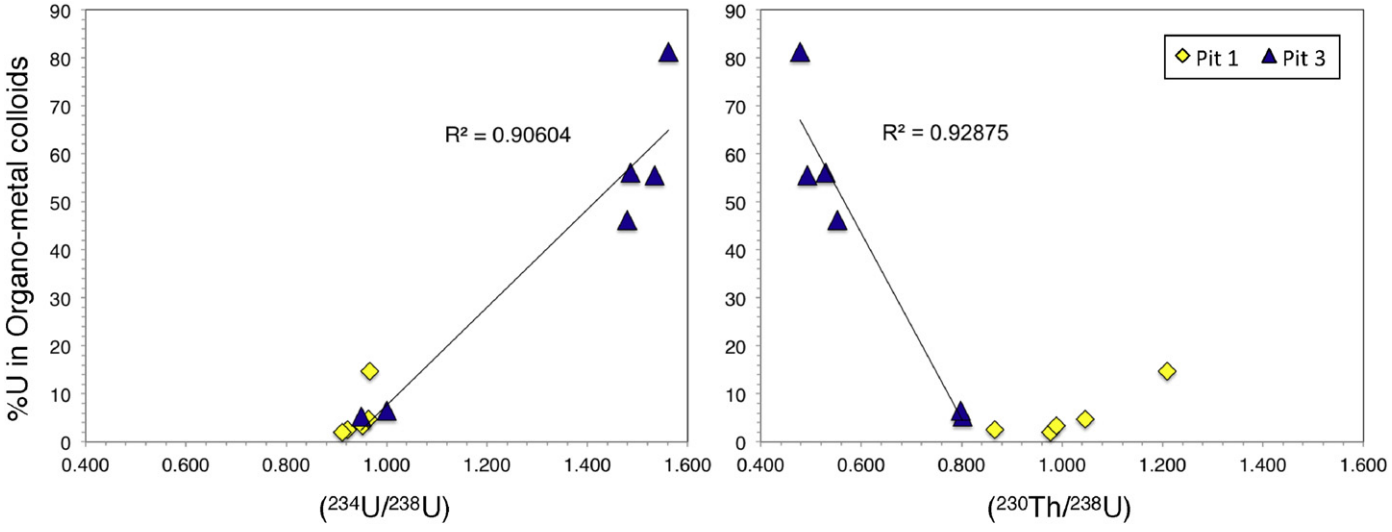

Fig. 9. Strong correlation is observed between (^{234}U/^{238}U) and (^{230}Th/^{238}U) with percent of U measured in Organo-metal colloids in samples from pit 3. Correlation is not observed in samples from pit 1.

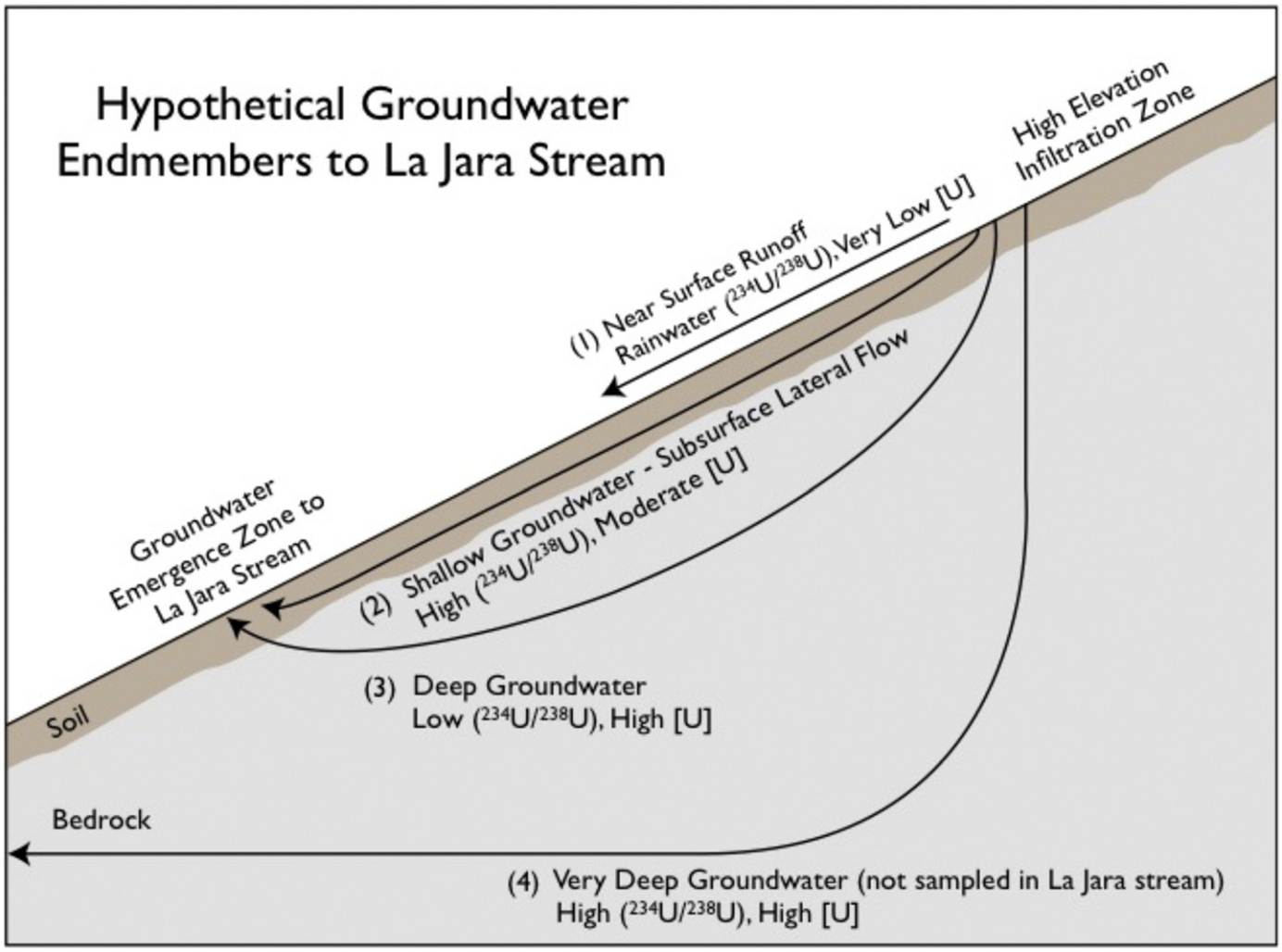

Fig. 11. Conceptual model describing hypothetical groundwater endmembers contributing to La Jara streamflow. La Jara streamwater is composed of a mixture between shallow groundwater and deep groundwater as shown above, the fractional contribution of these sources vary seasonally and longitudinally downstream. See Table 5 for full end-member description.

connection of subsurface flow paths and enabling more deep groundwater discharge into La Jara stream (Porter, 2012). The rising water table may also hydrologically connect shallower subsurface flow paths, resulting in flushing of DOC and solutes derived from shallow soils to stream flow (e.g. McGlynn and McDonnell, 2003; Pacific et al., 2010; Pedrial et al., 2014). During the rest of the year, stream flow is at low flow condition and controlled by a mixture of mostly shallow groundwater with smaller influence of deeper groundwater (Porter, 2012). Spatially, with the increase of drainage area downstream, the contributions of groundwater from various flowpaths to the stream become more significant (Liu et al., 2008a; Frisbee et al., 2012). In addition, these hydrologic processes play important roles in controlling the fate and transport of trace metals (e.g., trivalent lanthanides) through organic matter complexation and secondary mineral colloids in the La Jara catchment (Vazquez-Ortega et al., 2015a, 2016).

Both seasonal and spatial variations in ($^{234}U/^{238}U$) ratios were systematically observed in springs and along La Jara stream: 1) ($^{234}U/^{238}U$) values are on average 20% lower during the spring snowmelt season than those observed during the fall dry season; 2) longitudinal samples along La Jara stream show decreasing ($^{234}U/^{238}U$) ratios with decreasing elevation in both seasons (Fig. 5). Indeed, using Si as a proxy for deep groundwater contributions, we observe a strong negative correlation ($r^2 = 0.69$) between Si concentrations and ($^{234}U/^{238}U$) ratios in La Jara stream and springs for both seasons (Fig. 10), with only one exception for the South spring. Compared to other water samples, the South spring samples show elevated ($^{234}U/^{238}U$) ratios without a corresponding lower Si concentrations (Fig. 10). There are no differences in major ion

Table 5
Hypothetical groundwater endmembers to La Jara stream.

Endmember	Transit time	Dissolved load	U signature
1) Near surface runoff (very small contribution)	Very short	Low	Rainwater-like ($^{234}U/^{238}U$), very low U concentration
2) Shallow groundwater — lateral subsurface flow	Short	Moderate	High ($^{234}U/^{238}U$), low U concentration
3) Deep groundwater	Long	High	Low ($^{234}U/^{238}U$), high U concentration
4) Very deep groundwater (not sampled by La Jara stream or springs)	Very long	High	High ($^{234}U/^{238}U$) due to enhanced alpha recoil from aquifer matrix at depth, low U concentration

chemistry to provide evidence for why the South spring samples show a different Si vs. ($^{234}U/^{238}U$) trend. Although the South spring samples do not fit the general trend with all other La Jara samples, they do show similar seasonal variations, with lower ($^{234}U/^{238}U$) ratios and higher concentrations during the snowmelt season (Fig. 10).

The reduction in ($^{234}U/^{238}U$) ratios in springs and streams during the snowmelt season with greater contribution of deep groundwater suggests that the deep groundwater water end-member at La Jara is not characterized by an unusually high ($^{234}U/^{238}U$) signature as seen in other studies (e.g. Riotte et al., 2003; Bagard et al., 2011; Schaffhauser et al., 2014), but instead with a low ($^{234}U/^{238}U$) signature. Consistent with this inference, the trend of decreasing ($^{234}U/^{238}U$) ratios downstream in La Jara suggests increasing contributions of deep groundwater, with longer flow paths and residence time, but with lower ($^{234}U/^{238}U$) ratios, discharging to the stream at progressively lower elevations. Indeed, the Redondo Meadow spring, located outside the La Jara catchment, has been previously shown to best represent the deep groundwater end-member contributing to La Jara stream (with its high Si concentrations and inferred long residence time; Porter, 2012; Zapata-Rios et al., 2015a). The Redondo Meadow spring sample collected during the snowmelt season in 2012 has the lowest ($^{234}U/^{238}U$) value (1.68) observed in springs in this study (Fig. 5).

By contrast, the South spring, located at high elevation, has the highest observed ($^{234}U/^{238}U$) values (2.84 to 3.09; Fig. 5), suggesting it may represent the shallow groundwater end-member with short residence time and flow path but affected by easily released ^{234}U from recoil tracts in U-bearing mineral surfaces (Andersen et al., 2009). The observation of high ($^{234}U/^{238}U$) associated with short water residence time/flow path water at La Jara catchment can be linked to its unique hydrologic setting (Fig. 11; Table 5). The well-drained soils at the high elevation areas of the catchment prevent the generation of overland runoff and facilitate infiltration of snowmelt and rainwater. The combination of high infiltration and low hydraulic conductivity of the bedrock generates subsurface lateral flows along the soil-bedrock interface (Liu et al., 2008a). The subsurface lateral flow component is comprised of dilute water, undersaturated with respect to bedrock primary minerals (Zapata-Rios et al., 2015a, 2015b). It is hypothesized that the alpha recoil effect from fresh bedrock generates very high ($^{234}U/^{238}U$) ratios in the subsurface lateral flow component (shallow groundwater end-member with short water residence time; Fig. 11). Conversely, in the deep groundwater end-member with greater water residence time and longer flow path, chemical dissolution dominates U isotope fractionation resulting in lower ($^{234}U/^{238}U$) (Fig. 11).

Both the temporal and spatial variations of ($^{234}U/^{238}U$) in La Jara springs and stream water are consistent with the changing contributions of the two main water sources (shallow and deep groundwater) as suggested by previous studies (Broxton et al., 2009; Liu et al., 2008a, 2008b; Porter, 2012). Thus, at the catchment scale, we hypothesize that the subsurface lateral flow component (or the shallow groundwater component) at high elevation areas is characterized by high ($^{234}U/^{238}U$) due to enhanced alpha recoil effect at the soil-bedrock interface with a relatively short residence time, and the longer residence time waters in La Jara (e.g., the relatively deep groundwater end member at low elevation) generate lower ($^{234}U/^{238}U$) due to more extensive chemical dissolution (Fig. 11). Such a hypothesis is supported by laboratory studies on fresh granite dissolution in which high ($^{234}U/^{238}U$) in water phases were generated at the early stage of experiments and increasing duration of water-rock interaction resulted in waters with progressively lower ($^{234}U/^{238}U$) due to the depletion of more easily released ^{234}U from recoil tracts in U-bearing minerals (Andersen et al., 2009). Indeed, the fine volcanic ash deposits in the shallow horizons in our study area could be the source of relatively fresh materials for the enhanced alpha recoil effect to occur.

Such a hypothesis implies that, at the catchment scale, the different water residence time and flow path lengths are the main controlling factors for generating different ($^{234}U/^{238}U$) in subsurface lateral flow vs. groundwater end-members (or shallow vs. deep groundwater), assuming that other parameters such as grain sizes, water/rock surface ratio, and lithology remain the same in the subsurface environments. Such an assumption is difficult to test, as the physical properties of the aquifers from both water sources are not clearly known. However, the lithology of the La Jara Catchment remains relatively constant along the stream channel from Redondo peak to the La Jara catchment outlet (Fig. A1). In addition, the variations of ($^{234}U/^{238}U$) in stream waters were observed for both along the stream channels and for the same location in different hydrologic seasons. If the spatial variations were due to changes of subsurface parameters other than the water residence time, it would not generate the systematic seasonal variations as observed throughout the La Jara catchment. Hence, although we do not have direct evidence to discard the other controlling factors, we suggest that the water residence time and flow path are most likely the controlling factors for ($^{234}U/^{238}U$) in La Jara stream.

It is also noted that the West Fork spring, the highest elevation spring sampled in La Jara, exhibits a relatively low ($^{234}U/^{238}U$) value during both seasons (1.81 and 1.86). Despite its higher elevation relative to most of La Jara stream, it is possible that this spring discharges a greater proportion of relatively deeper groundwater compared to the South spring from outside catchment boundaries or via flow paths through less conductive porous media, potentially resulting in longer transit time groundwater with lower ($^{234}U/^{238}U$).

The decrease of ($^{234}U/^{238}U$) with increasing water residence time is in contrast to several recent studies that present evidence of increasing ($^{234}U/^{238}U$) with longer residence time waters in granitic spring waters due to an increasing contribution of ^{234}U during direct alpha recoil processes (e.g. Riotte et al., 2003; Bagard et al., 2011; Schaffhauser et al., 2014). Increasing ($^{234}U/^{238}U$) with increasing water-rock interaction have also been observed in deep groundwater environments (~km depth) such as in carbonate aquifers in Texas, which has been attributed to (1) precipitation of U from groundwater to aquifer surfaces due to change of redox conditions and (2) enhanced transfer of alpha-recoil ^{234}U from U-rich aquifer rock surfaces back to U-depleted groundwater (Kronfeld, 1974; Kronfeld et al., 1994). The observation that the relatively deep groundwater end-member in La Jara has lower ($^{234}U/^{238}U$) suggests that (1) chemical dissolution dominates U isotope fractionation during subsurface water-rock interaction in La Jara, as evidenced by the observation that water in La Jara is undersaturated with respect to bedrock primary minerals (Zapata-Rios et al., 2015a, 2015b), and (2) alpha recoil effects were not enhanced in the subsurface of La Jara, probably due to a lack of U-rich mineral surfaces at the shallow depth. Different subsurface environmental conditions (water saturation index, redox conditions, organic matter content, and available particle surfaces for U precipitation) may have generated a different U isotope fractionation trend in the deep groundwater end-member of the La Jara catchment relative to the granitic catchment in France and the carbonate aquifer in Texas (Kronfeld, 1974; Kronfeld et al., 1994; Schaffhauser et al., 2014). However, other hypothetical deep groundwater end-members characterized by much longer water residence time and higher ($^{234}U/^{238}U$) ratio may exist at greater depths within the Valles Caldera but may not contribute to the stream flow in the La Jara catchment (e.g. Fig. 11).

7. Conclusions

Analysis of U-series isotopes in weathering profiles in the complex volcanic terrain of the Valles Caldera reveals U-series depth trends unlike those expected from simple weathering profiles: e.g. ($^{234}U/^{238}U$) and ($^{230}Th/^{238}U$) decrease and increase towards surface, respectively. A dominant process controlling the U-series composition of soils in the La Jara ZOB is mixing with volcanic ash and atmospheric dust, rather than chemical weathering alone. Due to episodic mixing with volcanic ash and dust, and large-scale soil solid phase heterogeneity in the ZOB landscape, modeling soil formation using an existing U-series model

that assumes soil production from a single parent and constant inputs of U-series isotopes over time is not appropriate for this landscape. U-series isotopes show promise for use in identifying fractional contributions of dust and volcanic ash to the U and Th mass budget of similar soils in future studies. Significant ^{234}U enrichment in one soil profile was interpreted as evidence of addition of U to soils from ^{234}U-enriched soil solutions. Soil sequential extraction confirms that most of the U is contained in organo-metal colloid and exchangeable forms in shallow soils of this profile.

Dissolved ($^{234}U/^{238}U$) values measured in spring and stream waters in La Jara catchment show systematic variation between spring snowmelt and fall dry seasons, consistent with previous studies at the site, as well as longitudinally along La Jara stream. Our results suggest that the variations in ($^{234}U/^{238}U$) in La Jara surface waters may reflect changes in contribution of deep vs. shallow groundwater sources, each with their own distinct ($^{234}U/^{238}U$), which combine to regulate the ($^{234}U/^{238}U$) measured along La Jara stream and at the catchment outlet. We hypothesize that residence time may control the ($^{234}U/^{238}U$) of these source waters (Fig. 11) and further studies using more quantitative age tracers, such as ^{3}H, could verify the relative residence time of these source waters in La Jara. If established, ($^{234}U/^{238}U$) values could be a powerful tracer of water sources and residence time at the catchment scale.

Supplementary data to this article can be found online at http://dx.doi.org/10.1016/j.chemgeo.2016.04.003.

Acknowledgments

This research was supported by the Santa Catalina-Jemez River Basin Critical Zone Observatory funded by NSF grants EAR-0724958 and EAR-1331408. Funding was also provided by NSF grants EAR-1349056 (J.M.), EAR-1349091 (L.M), and EAR/IF-0929850. Analytical and fieldwork expenses were partially supported by SAHRA and the University of Arizona GPSC. The following people assisted with fieldwork and laboratory analyses: Juliana Loaiza, Mercer Meding, Syprose Nyachoti, Adrian Harpold, Xavier Zapata-Rios, Scott Compton, Julia Perdrial, Mary Kay Amistadi, Tim Corley, Matej Duric, Courtney Porter, and David Vinson.

References

Andersen, M.B., Stirling, C.H., Porcelli, D., Halliday, A.H., Andersson, P.S., Baskaran, M., 2007. The tracing of riverine U in Arctic seawater with very precise $^{234}U/^{238}U$ measurements. Earth Planet. Sci. Lett 259, 171–185.

Andersen, M.B., Erel, Y., Bourdon, B., 2009. Experimental evidence for U-234–U-238 fractionation during granite weathering with implications for U-234/U-238 in natural waters. Geochim. Cosmochim. Acta 73 (14), 4124–4141.

Andersen, M.B., Vance, D., Keech, A., Rickli, J., Hudson, G., 2013. Estimating U fluxes in a high-latitude, boreal post-glacial setting using U-series isotopes in soils and rivers. Chem. Geol. 354, 22–33.

Anderson, S.P., Dietrich, W.E., Brimhall, G.H., 2002. Weathering profiles, mass-balance analysis, and rates of solute loss: linkages between weathering and erosion in a small, steep catchment. GSA Bull. 114 (9), 1143–1158.

Asmerom, Y., 1999. Th–U fractionation and mantle structure. Earth Planet. Sci. Lett. 166 (3–4), 163–175.

Bagard, M.-L., Chabaux, F., Pokrovsky, O.S., Viers, J., Prokushkin, A.S., Stille, P., Rihs, S., Schmitt, A.-D., Dupre, B., 2011. Seasonal variability of element fluxes in two Central Siberian rivers draining high latitude permafrost dominated areas. Geochim. Cosmochim. Acta 75, 3335–3357.

Berner, R.A., Lasaga, A., Garrels, R.M., 1983. The carbonate–silicate geochemical cycle and its effect on atmospheric carbon dioxide over the past 100 million years. Am. J. Sci. 283, 641–683.

Bourdon, B., Bureau, S., Andersen, M.B., Pili, E., Hubert, A., 2009. Weathering rates from top to bottom in a carbonate environment. Chem. Geol. 258 (3–4), 275–287.

Brantley, S.L., Goldhaber, M.B., Ragnarsdottir, K.V., 2007. Crossing disciplines and scales to understand the critical zone. Elements 3 (5), 307–314.

Brimhall, G.H., Dietrich, W.E., 1987. Constitutive mass balance relations between chemical composition, volume, density, porosity, and strain in metasomatic hydrochemical systems: results on weathering and pedogenesis. Geochim. Cosmochim. Acta 51, 567–587.

Broxton, P.D., Troch, P.A., Lyon, S.W., 2009. On the role of aspect to quantify water transit times in small mountainous catchments. Water Resour. Res. 45, W08427.

Capo, R.C., Chadwick, O.A., 1999. Sources of strontium and calcium in desert soil and calcite. Earth Planet. Sci. Lett. 170, 61–72.

Chabaux, F., Dequincey, O., Leveque, J., Leprun, J., Clauer, N., Riotte, J., Paquet, H., 2003a. Tracing and dating recent chemical transfers in weathering profiles by trace-element geochemistry and U-238–U-234–Th-230 disequilibria: the example of the Kaya lateritic toposequence (Burkina-Faso). Compt. Rendus Geosci. 335 (16), 1219–1231.

Chabaux, F., Riotte, J., Dequincey, O., 2003b. U–Th–Ra fractionation during weathering and river transport. Rev. Mineral. Geochem. 52, 533–576.

Chabaux, F., Bourdon, B., Riotte, J., 2008. Chapter 3 U-series geochemistry in weathering profiles, river waters and lakes. Radioact. Environ. 13, 49–104 (Elsevier).

Chabaux, F., Ma, L., Stille, P., Pelt, E., Granet, M., Lemarchand, D., Roupert, R.d.C., Brantley, S.L., 2011. Determination of chemical weathering rates from U series nuclides in soils and weathering profiles: principles, applications and limitations. Appl. Geochem. 26, S20–S23.

Chabaux, F., Blaes, E., Stille, P., Roupert, R.D., Pelt, E., Dosseto, A., Ma, L., Buss, H.L., Brantley, S.L., 2013. Regolith formation rate from U-series nuclides: implications from the study of a spheroidal weathering profile in the Rio Icacos watershed (Puerto Rico). Geochim. Cosmochim. Acta http://dx.doi.org/10.1016/j.gca.2012.09.037.

Chorover, J., Vitousek, P.M., Everson, D.A., Esperanza, A.M., Turner, D., 1994. Solution chemistry profiles of mixed-conifer forests before and after fire. Biogeochemistry 26, 115–144.

Chorover, J., Troch, P.A., Rasmussen, C., Brooks, P.D., Pelletier, J.D., Breshears, D.D., Huxman, T.E., Kurc, S.A., Lohse, K.A., McIntosh, J.C., Meixner, T., Schaap, M.G., Litvak, M.E., Perdrial, J., Harpold, A., Durcik, M., 2011. How water, carbon, and energy drive critical zone evolution: the Jemez-Santa Catalina critical zone observatory. Vadose Zone J. 10 (3), 884–899.

DePaolo, D.J., Maher, K., Christensen, J.N., McManus, J., 2006. Sediment transport time measured with U-series isotopes: results from ODP North Atlantic drift site 984. Earth Planet. Sci. Lett. 248, 394–410.

Dequincey, O., Chabaux, F., Clauer, N., Sigmarsson, O., Liewig, N., Leprun, J.C., 2002. Chemical mobilizations in laterites: evidence from trace elements and U-238–U-234–Th-230 disequilibria. Geochim. Cosmochim. Acta 66 (7), 1197–1210.

Dosseto, A., Turner, S.P., Chappell, J., 2008. The evolution of weathering profiles through time: new insights from uranium-series isotopes. Earth Planet. Sci. Lett. 274 (3–4), 359–371.

Dosseto, A., Buss, H., Suresh, P.O., 2011. The delicate balance between soil production and erosion, and its role on landscape evolution. Appl. Geochem. 26, S24–S27.

Dosseto, A., Buss, H.L., Suresh, P.O., 2012. Rapid regolith formation over volcanic bedrock and implications for landscape evolution. Earth Planet. Sci. Lett. 337, 47–55.

Drever, J.I., 1997. The Geochemistry of Natural Waters: Surface and Groundwater Environments ISBN-10:0132727900.

Durand, S., Chabaux, F., Rihs, S., Duringer, P., Elsass, P., 2005. U isotope ratios as tracers of groundwater inputs into surface waters: example of the Upper Rhine hydrosystem. Chem. Geol. 220 (1–2), 1–19.

Fleischer, R.L., 1982. Alpha-recoil damage and solution effects in minerals — uranium isotopic disequilibrium and radon release. Geochim. Cosmochim. Acta 46 (11), 2191–2201.

Frisbee, M.D., Phillips, F.M., Weissmann, G.S., Brooks, P.D., Wilson, J.L., Campell, A.R., Liu, F., 2012. Unraveling the mysteries of the large watershed black box: implications for the streamflow response to climate and landscape perturbations. Geophys. Res. Lett. 39, L01404. http://dx.doi.org/10.1029/2011GL050416.

Gaillardet, J., Viers, J., Dupre, B., 2005. Trace elements in river waters. Treatise on geochemistry. Surf. Ground Water Weather. Soils 5, 225–272.

Goff, F., 2009. Valles Caldera: A Geologic History. TWP America, Inc., Singapore.

Gustafson, J.R., Brooks, P.D., Molotch, N.P., Veatch, W.C., 2010. Estimating snow sublimation using natural chemical and isotopic tracers across a gradient of solar radiation. Water Resour. Res. 46, W12511.

Handley, H., Turner, S., Dosseto, A., Haberlah, D., Afonso, J., 2013. Considerations for U-series dating of sediments: insights from the Flinders Ranges, South Australia. Chem. Geol. 340, 40–48.

Hodge, V.F., Johannesson, K.H., Stetzenbach, K.J., 1996. Rhenium, molybdenum, and uranium in groundwater from the southern Great Basin, USA: evidence for conservative behavior. Geochim. Cosmochim. Acta 60, 3197–3214.

Keech, A.R., West, A.J., Pett-Ridge, J.C., Henderson, G.M., 2013. Evaluating U-series tools for weathering rate and duration on a soil sequence of known ages. Earth Planet. Sci. Lett. 274, 24–35.

Kirchner, J.W., Tetzlaff, D., Soulsby, C., 2010. Comparing chloride and water isotopes as hydrological tracers in two Scottish catchments. Hydrol. Process. 24 (12), 1631–1645.

Kronfeld, J., 1974. Uranium deposition and Th-234 alpha-recoil: an explanation for extreme 234U/238U fractionation within the Trinity aquifer. Earth Planet. Sci. Lett. 21, 327–330.

Kronfeld, J., Vogel, J.C., 1991. Uranium isotopes in surface waters from Southern Africa. Earth Planet. Sci. Lett. 105 (1–3), 191–195.

Kronfeld, J., Vogel, J.C., Talma, A.S., 1994. A new explanation for extreme 234U/238U disequilibria in a dolomitic aquifer. Earth Planet. Sci. Lett. 123, 81–93.

Land, M., Ohlander, B., Ingri, J., Thunberg, J., 1999. Solid speciation and fractionation of rare earth elements in a spodosol profile from northern Sweden as revealed by sequential extraction. Chem. Geol. 160 (1–2), 121–138.

Langmuir, D., 1997. Aqueous Environmental Geochemistry. Prentice Hall, Upper Saddle River, N.J.

Laveuf, C., Cornu, S., Guilherme, L.R.G., Guerin, A., Juillot, F., 2012. The impact of redox conditions on the rare earth element signature of redoximorphic features in a soil sequence developed from limestone. Geoderma 170, 25–38.

Lavoie, M., Starr, G., Mack, M.C., Martin, T.A., Gholz, H.L., 2010. Effects of a prescribed fire on understory vegetation, carbon pools, and soil nutrients in a longleaf pine-slash pine forest in Florida. Nat. Areas J. 30 (1), 82–94.

Liu, F., Bales, R.C., Conklin, M.H., Conrad, M.E., 2008a. Streamflow generation from snowmelt in semi-arid, seasonally snow-covered, forested catchments, Valles Caldera, New Mexico. Water Resour. Res. 44 (12), W12443.

Liu, F., Parmenter, R., Brooks, P.D., Conklin, M.H., Bales, R.C., 2008b. Seasonal and interannual variation of streamflow pathways and biogeochemical implications in semi-arid, forested catchments in Valles Caldera, New Mexico. Ecohydrology 1 (3), 239–252.
Ma, L., Chabaux, F., Pelt, E., Blaes, E., Jin, L., Brantley, S., 2010. Regolith production rates calculated with uranium-series isotopes at Susquehanna/Shale Hills Critical Zone Observatory. Earth Planet. Sci. Lett. 297 (1–2), 211–225.
Ma, L., Chabaux, F., West, N., Kirby, E., Jin, L., Brantley, S.L., 2013. Regolith production and transport in the Susquehanna Shale Hills Critical Zone Observatory, part 1: insights from U-series isotopes. J. Geophys. Res. Earth Surf. 118, 722–740. http://dx.doi.org/10.1002/jgrf.20037.
Maher, K., 2011. The role of fluid residence time and topographic scales in determining chemical fluxes from landscapes. Earth Planet. Sci. Lett. 312 (1–2), 48–58.
Maher, K., Steefel, C.I., DePaolo, D.J., Viani, B.E., 2006. The mineral dissolution rate conundrum: insights from reactive transport modelling of U isotopes and pore fluid chemistry in marine sediments. Geochim. Cosmochim. Acta 70, 337–363.
Maher, K., Ibarra, D., Oster, J., Miller, D., Redwine, J., Reheis, M., Harden, J., 2014. Uranium isotopes in soils as a proxy for past infiltration and precipitation across the western United States. Am. J. Sci. 314, 821–857.
Mathieu, D., Bernat, M., Nahon, D., 1995. Short-lived U and Th isotope distribution in a tropical laterite derived from granite (Pitinga river basin, Amazonia, Brazil): application to assessment of weathering rate. Earth Planet. Sci. Lett. 136 (3–4), 703–714.
McGlynn, B.L., McDonnell, J.J., 2003. Role of discrete landscape units in controlling catchment dissolved organic carbon dynamics. Water Resour. Res. 39 (4), 1090.
McGuire, K.J., McDonnell, J.J., 2006. A review and evaluation of catchment transit time modeling. J. Hydrol. 330 (3–4), 543–563.
Montgomery, D.R., 2007. Soil erosion and agricultural sustainability. Proc. Natl. Acad. Sci. U. S. A. 104 (33), 13268–13272.
Muldavin, E., Tonne, P., 2003a. A Vegetation Survey and Preliminary Ecological Assessment of Valles Caldera National Preserve, New Mexico: Report for Cooperative Agreement No. 01CRAG0014. University of New Mexico, Albuquerque.
Muldavin, E., Tonne, P., 2003b. A Vegetation Survey and Preliminary Ecological Assessment of Valles Caldera National Preserve, New Mexico, Albuquerque, Natural Heritage.
Nauret, F., Hemond, C., Maury, R.C., Aguillon-Robles, A., Guillou, H., Le Faouder, A., 2012. Extreme Th-230 excesses in magnesian andesites from Baja California. Lithos 146, 143–151.
Osmond, J.K., Cowart, J.B., 1992. Ground water. In: Ivanovich, M, Harmon, R.S. (Eds.), Uranium-series disequilibrium. Clarendon Press Oxford, pp. 290–334.
Oster, J.L., Ibarra, D.E., Harris, C.R., Maher, K., 2012. Influence of eolian deposition and rainfall amounts on the U-isotopic composition of soil water and soil minerals. Geochim. Cosmochim. Acta 88, 146–166.
Pacific, V.J., Jencso, K.G., McGlynn, B.L., 2010. Variable flushing mechanisms and landscape structure control stream DOC export during snowmelt in a set of nested catchments. Biogeochemistry 99 (1–3), 193–211.
Pedrial, J.N., Perdrial, N., Vazquez-Ortega, A., Porter, C., Leedy, J., Chorover, J., 2014. Experimental assessment of passive capillary wick sampler suitability for inorganic soil solution constituents. Soil Sci. Soc. Am. J. 78 (2), 486–495.
Pelt, E., Chabaux, F., Innocent, C., Navarre-Sitchler, A.K., Sak, P.B., Brantley, S.L., 2008. Uranium-thorium chronometry of weathering rinds: rock alteration rate and paleoisotopic record of weathering fluids. Earth Planet. Sci. Lett. 276 (1–2), 98–105.
Pelt, E., Chabaux, F., Stille, P., Innocent, C., Ghaleb, B., Gerard, M., Guntzer, F., 2013. Atmospheric dust contribution to the budget of U-series nuclides in soils from the Mount Cameroon volcano. Chem. Geol. 341, 147–157.
Perdrial, J.N., Perdrial, N., Harpold, A., Gao, X., Gabor, R., LaSharr, K., Chorover, J., 2012. Impacts of sampling dissolved organic matter with passive capillary wicks versus aqueous soil extraction. Soil Sci. Soc. Am. J. 76 (6), 2019–2030.
Plater, A., Dugdale, R., Ivanovich, M., 1994. Sediment yield determination using uranium-series radionuclides — the case of the Wash and Fenland drainage-basin, eastern England. Geomorphology 11 (1), 41–56.
Pogge von Strandmann, P.A.E., Burton, K.w., James, R.H., van Calsteren, P., Gislason, S.R., 2010. Assessing the role of climate on uranium and lithium isotope behavior in rivers draining a basaltic terrain. Chem. Geol. 270, 227–239.
Porcelli, D., Swarzenski, P.W., 2003. The behavior of U-and Th-series nuclides in groundwater. Rev. Mineral. Geochem. 52 (1), 317–361.
Porter, C., 2012. Solute inputs to soil and stream waters in a seasonally snow-covered mountain catchment determined using Ge/Si, $^{87}SR/^{86}SR$ and major ion chemistry: Valles Caldera, New Mexico (Unpublished master's thesis) The University of Arizona, Tucson, Arizona.
Rasmussen, C., Meding, S.M., Vazquez-Ortega, A., Chorover, J., 2012. Domes, ash, and dust: controls on soil genesis in a montane catchment of the Valles Caldera. Oral Presentation. American Geophysical Union Fall Meeting.
Riotte, J., Chabaux, F., 1999. U-234/U-238) activity ratios in freshwaters as tracers of hydrological processes: the Strengbach watershed (Vosges, France). Geochim. Cosmochim. Acta 63 (9), 1263–1275.
Riotte, J., Chabaux, F., Benedetti, M., Dia, A., Boulègue, J., Gérard, M., Etamè, J., 2003. ^{234}U-^{238}U fractionations in surface waters: the Mount Cameroun case. Chem. Geol. 202, 365–381.
Robinson, L.F., Henderson, G.M., Hall, L., Matthews, I., 2004. Climatic control of riverine and seawater uranium-isotope ratios. Science 305 (5685), 851–854.
Russo, C.J., Rubin, K.H., Graham, D.W., 2009. Mantle melting and magma supply to the Southeast Indian Ridge: the roles of lithology and melting conditions from U-series disequilibria. Earth Planet. Sci. Lett. 278 (1–2), 55–66.
Schaffhauser, T., Chabaux, F., Ambroise, B., Lucas, Y., Stille, P., Reuschlé, T., Perrone, T., Fritz, B., 2014. Geochemical and isotopic (U, Sr) tracing of water pathways in the small granitic Ringelbach catchment (Vosges Mountains, France). Chem. Geol. 374-375, 117–127.
Sims, K.W.W., Gill, J.B., Dosseto, A., Hoffmann, D.L., Lundstrom, C.C., Williams, R.W., Ball, L., Tollstrup, D., Turner, S., Prytulak, J., Glessner, J.G., Standish, J.J., Elliott, T., 2008. An inter-laboratory assessment of the thorium isotopic composition of synthetic and rock reference materials. Geostand. Geoanal. Res. 32, 65–91.
Tricca, A., Wasserburg, G.J., Porcelli, D., Baskaran, M., 2001. The transport of U- and Th-seriesnuclides in a sandy unconfined aquifer. Geochim. Cosmochim. Acta 65, 1187–1210.
Vazquez-Ortega, A., Perdrial, J., Harpold, A., Zapata, X., Rasmussen, C., McIntosh, J., Schaap, M., Pelletier, J.D., Brooks, P., Amistadi, M.K., Chorover, J., 2015a. Rare earth elements as reactive tracers of biogeochemical weathering in forested rhyolitic terrain. Chem. Geol. 391, 19–32.
Vázquez-Ortega, A., Huckle, D., Perdrial, J., Amistadi, M.K., Durcik, M., Rasmussen, C., McIntosh, J., Chorover, J., 2016. Solid-phase redistribution of rare earth elements in hillslope pedons subjected to different hydrologic fluxes. Chem. Geol. 426, 1–18.
Vigier, N., Bourdon, B., Turner, S., Allegre, C.J., 2001. Erosion timescales derived from U-decay series measurements in rivers. Earth Planet. Sci. Lett. 193 (3–4), 549–563.
Vigier, N., Burton, K.W., Gislason, S.R., Rogers, N.W., Duchene, S., Thomas, L., Hodge, E., Schaefer, B., 2006. The relationship between riverine U-series disequilibria and erosion rates in a basaltic terrain. Earth Planet. Sci. Lett. 249 (3–4), 258–273.
Wilkinson, B.H., McElroy, B.J., 2007. The impact of humans on continental erosion and sedimentation. Geol. Soc. Am. Bull. 119, 140–156.
Wolff, J.A., Brunstad, K.A., Gardner, J.N., 2011. Reconstruction of the most recent volcanic eruptions from the Valles caldera, New Mexico. J. Volcanol. Geotherm. Res. 199 (1–2), 53–68.
Zapata-Rios, X., McIntosh, J., Rademacher, L., Troch, P.A., Rasmussen, C., Chorover, J., 2015a. Climatic and landscape controls on water transit times and silicate mineral weathering in the critical zone. Water Resour. Res. http://dx.doi.org/10.1002/2015WR017018.
Zapata-Rios, X., Troch, P., McIntosh, J., Broxton, P., Harpold, A., Litvak, M., Brooks, P., 2015b. Influence of terrain aspect on water partitioning, vegetation structure, and vegetation greening in high elevation catchments in northern New Mexico. Ecohydrology http://dx.doi.org/10.1002/eco.1674.